HZB Helmholtz Zentrum Berlin

RF and DC characterization for R&D

Oliver Kugeler

EASISchool 3 – 28.9.2020 ... 9.10.2020 – Genoa, Italy

Outline

- Purpose of sample testing
- Background
- QPR (quadrupole resonator)
- other RF techniques & measurement examples
- DC techniques & measurement examples

Why sample characterisation?

Manufacturing perspective

- investigate alternative SRF materials
- optimize film-fabrication procedure
- avoid making full cavity with novel material/technique

→ start with flat, small surface – apply lessons learned to cavity

Scientific perspective

- explore parameter space not accessible to cavity

  (i.e. temperature, frequency, B-field)
- measure physical properties of new materials

  (critical fields, penetration depth, coherence length, etc.)

Glossary

Name	Symbol	Definition
critical temperature	T_c	temperature below which a superconductor exhibits superconductivity at zero magnetic field strength and zero electrical current
critical (magnetic) field strength	H_c	magnetic field strength corresponding to the superconducting condensation energy at zero magnetic field strength (is a function of temperature, calculated from thermodynamics)
lower critical (magnetic) field strength	H_{c1}	magnetic field strength at which a fluxon firstly penetrates a bulk type II superconductor deviating from the perfect diamagnetism when demagnetization factor is zero
upper critical (magnetic) field strength	H_{c2}	magnetic flux density that completely suppresses superconductivity in a type II superconductor
superheating (magnetic) field strength	H_{sh}	magnetic field up to which perfect diamagnetism persists metastably

Courtesy G. Ciovati

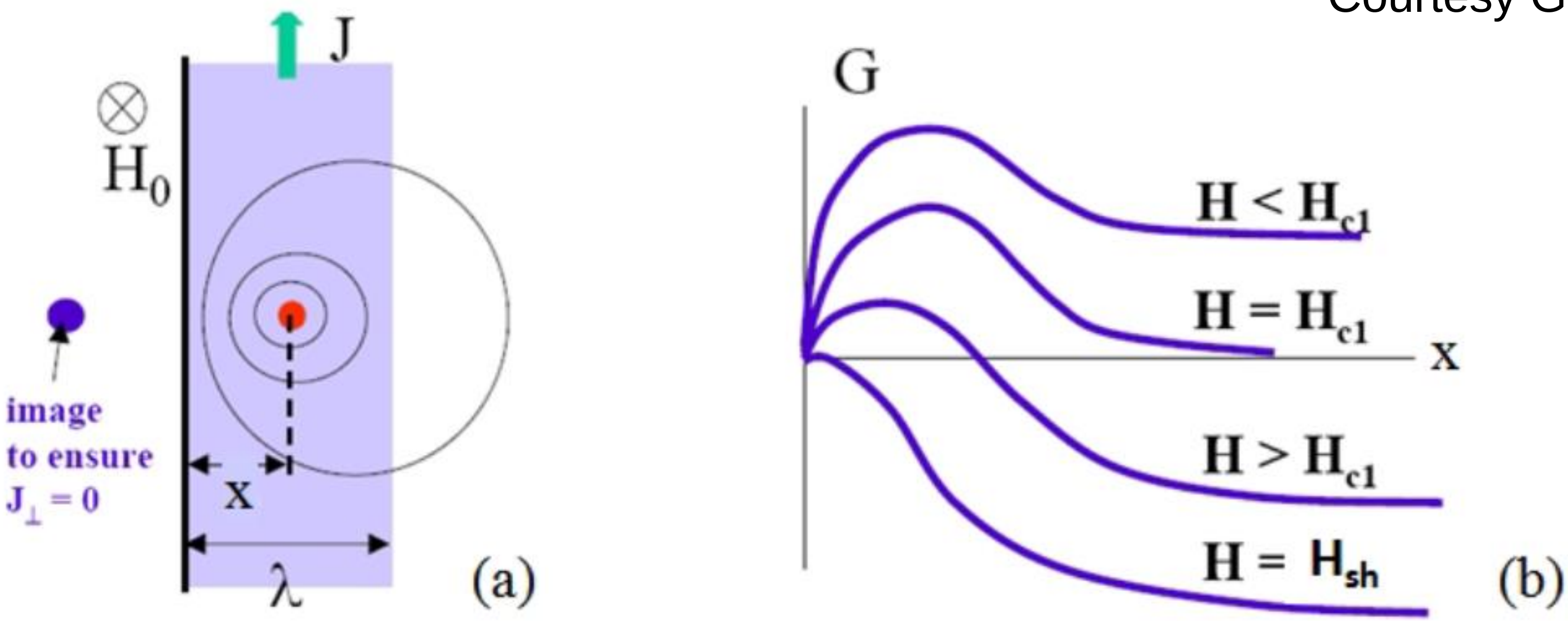

$$G(x) = \phi_0 \left[H_0 e^{-x/\lambda} - \frac{\phi_0}{4\pi\lambda^2} K_0\left(\frac{2x}{\lambda}\right) + H_{c1} - H_0 \right]$$

Gibbs free energy of single fluxoid as function of fluxoid position

BCS surface resistance $R_s \sim \sqrt{\rho_n}\ \exp\left(-{}^{\Delta}/_{k_b T}\right)$

need low nc resistivity and large energy gap

Material	T_c (K)	ρ_n(μΩcm)	$H_c(0)$ [T]	$H_{c1}(0)$ [T]	$H_{c2}(0)$ [T]	$\lambda(0)$ [nm]
Nb	9.2	2	0.2	0.17	0.4	40
NbN	16.2	70	0.23	0.02	15	200
NbTiN	17.5	35		0.03		151
Nb_3Sn	18	20	0.54	0.05	30	85
V_3Si	17					
Mo_3Re	15		0.43	0.03	3.5	140
MgB_2	40		0.43	0.03	3.5	140

$\Delta \sim T_c$; $\rho_n \sim \sqrt{\lambda(0)/T_c}$; $H_{sh}(0) \sim (0.745\ldots\ 1.2) * H_c(0)$

Courtesy S. Keckert

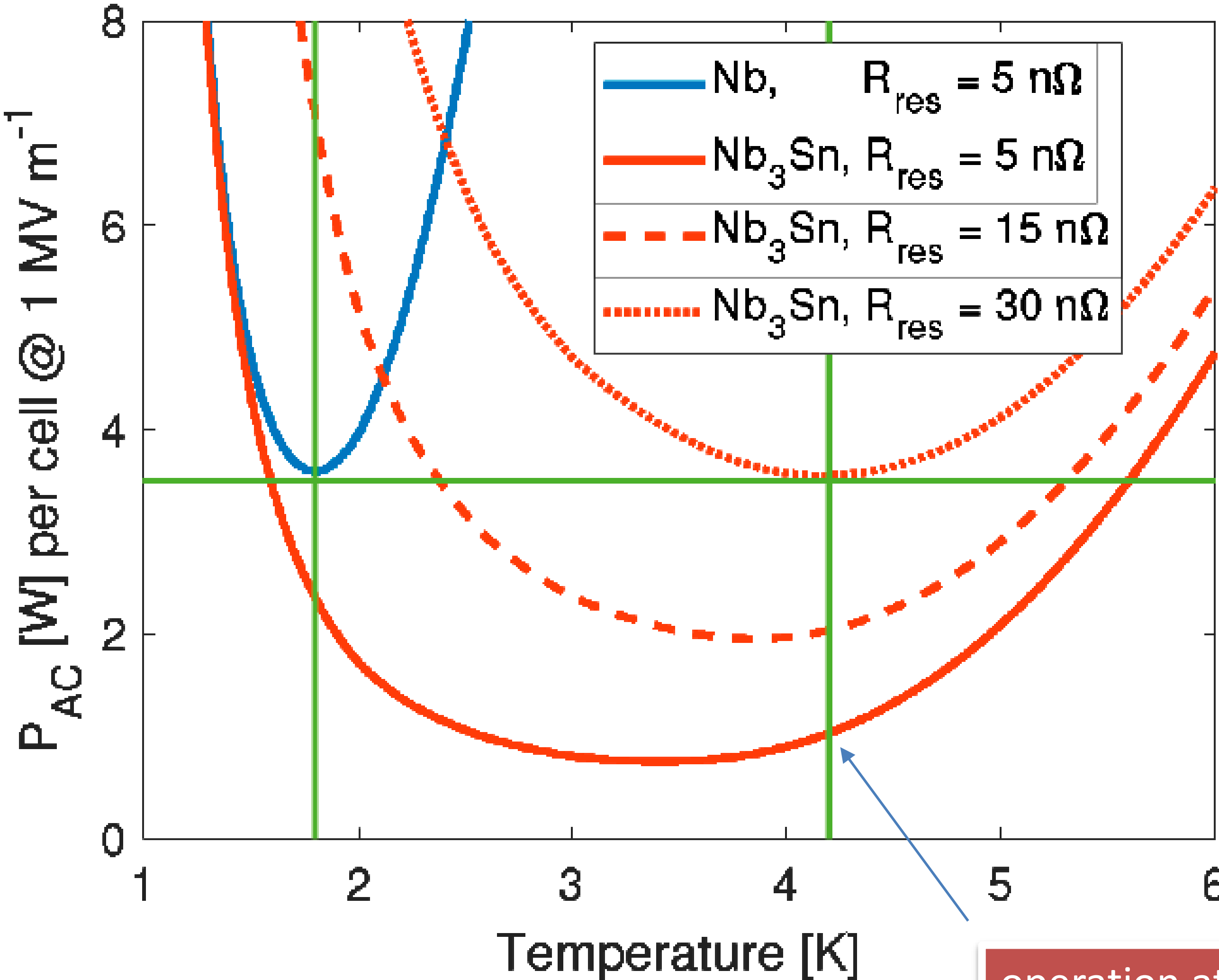

operation at LHe temperature possible

Courtesy S. Keckert

Modify the RF penetration behavior (+ new material)

[A. Gurevich, APL 88, 012511, 2006]

- Penetration depth $\lambda \approx 30 \ldots 300\ \mathrm{nm}$
  → Coatings are possible
- Thin films: $d < \lambda$
  → Distribute RF currents

→ Less RF field at the substrate
  → Reduced RF losses
  → Higher quench field

→ Prevents vortex avalanches
  → Stability

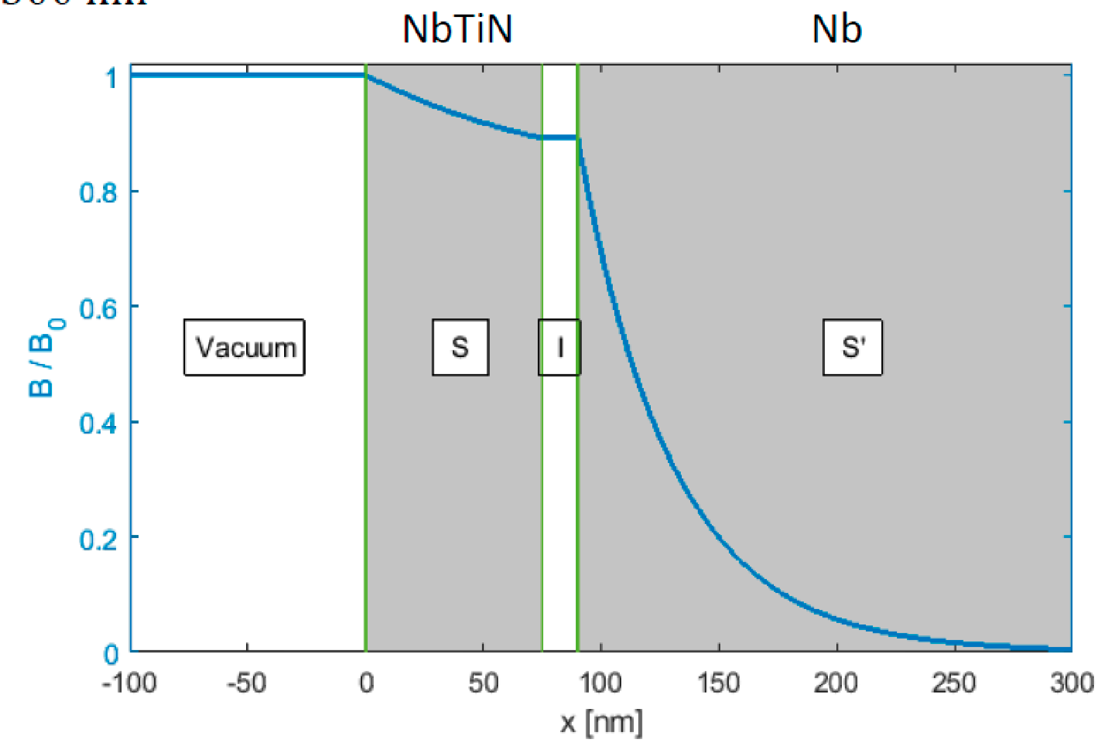

RF TECHNIQUES

Testing RF properties of sc samples follows two aims:

- test specific material for suitability for use in SRF cavity
- systematic testing of RF losses and other sc properties

How does an ideal experiment look like?

- Small and flat samples, easy to change
- Measure surface resistance in wide parameter space
  - wide temperature range, high RF field
  - multiple frequencies (~0.5 .. 2 GHz)
  - control of cooling conditions (magnetic flux studies)
- Penetration depth, critical field, transition temperature, RRR, thermal conductivity

DC resistance measurement

$$R = \frac{U}{I}$$

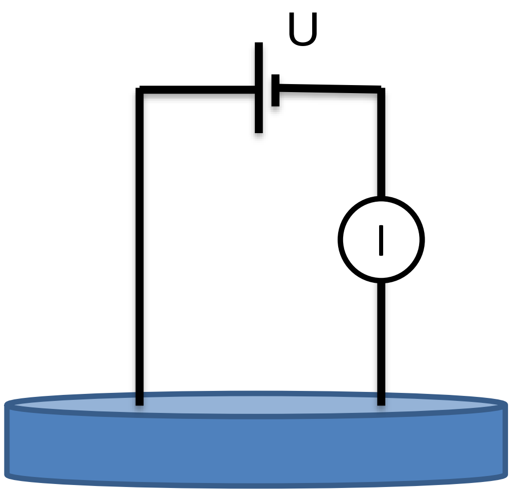

Problems:

- resolution ~100 μΩ, need nΩ
- need values at ~GHz frequency

AC measurement

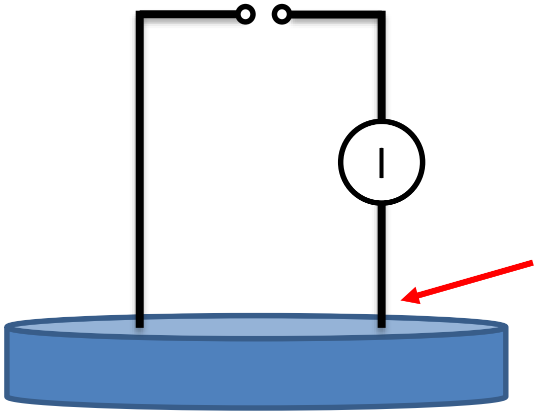

Impedance mismatch as frequency goes up.
Almost full reflection at GHz

Problem: How to get current into sample?

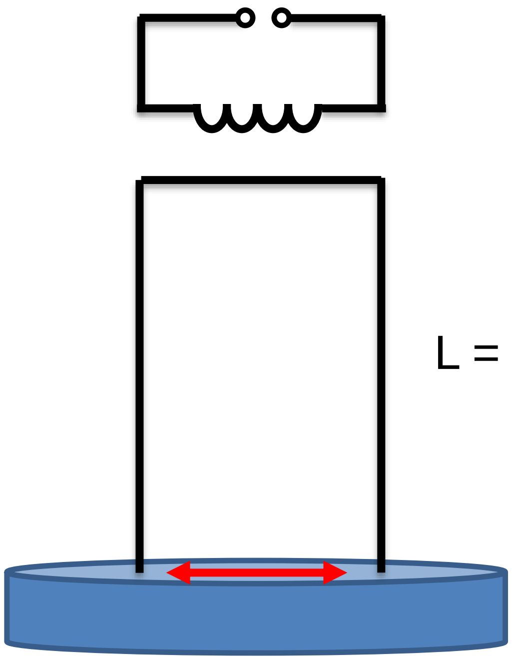

L = loop circumference

adjust wire length, use resonances $\lambda = \frac{c}{f} = n \times L$

supply by power coupling

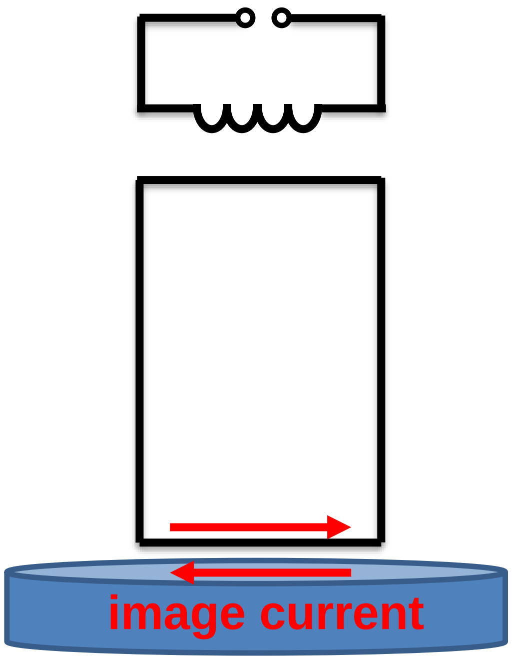

detach loop from sample
make use of image current

attachment of wires obsolete!

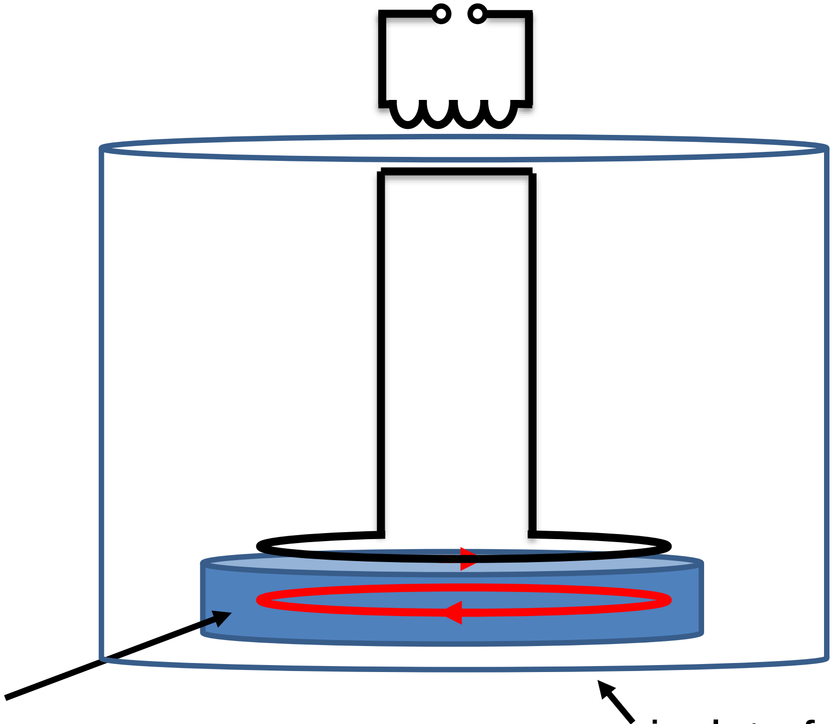

maximize exposure area

isolate from environment

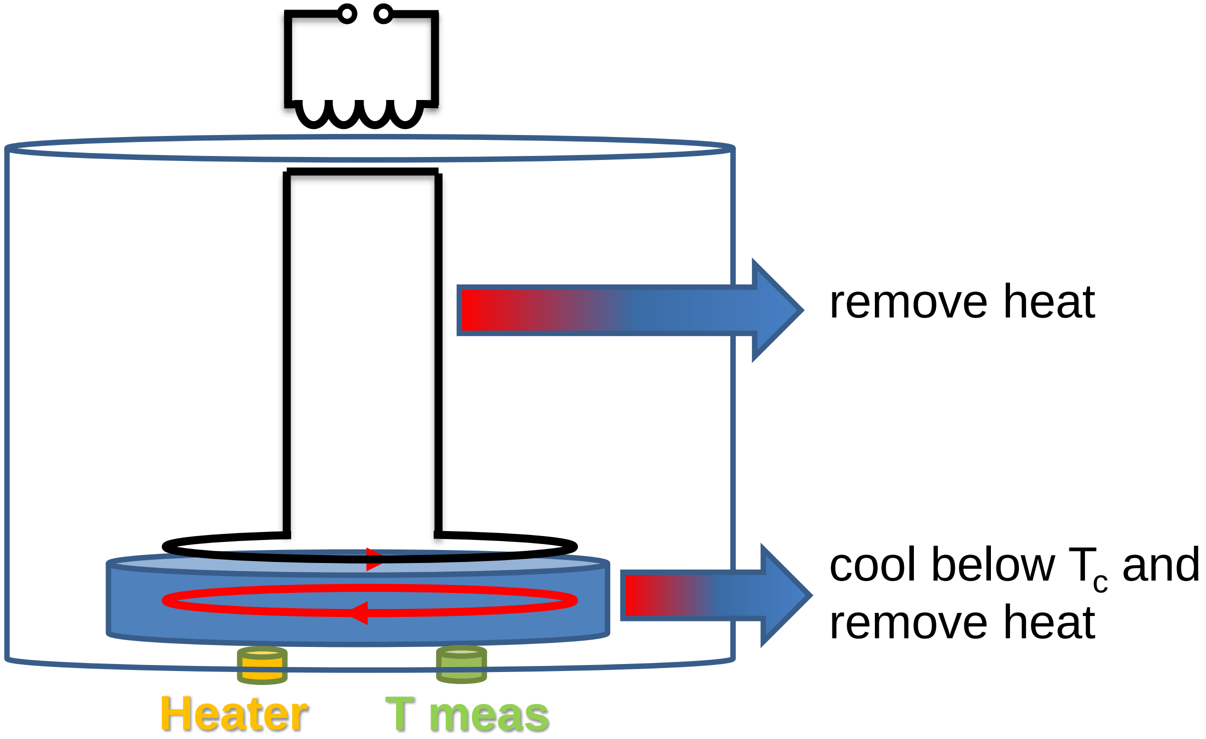

measure ΔT caused by RF
compare with ΔT caused by heater

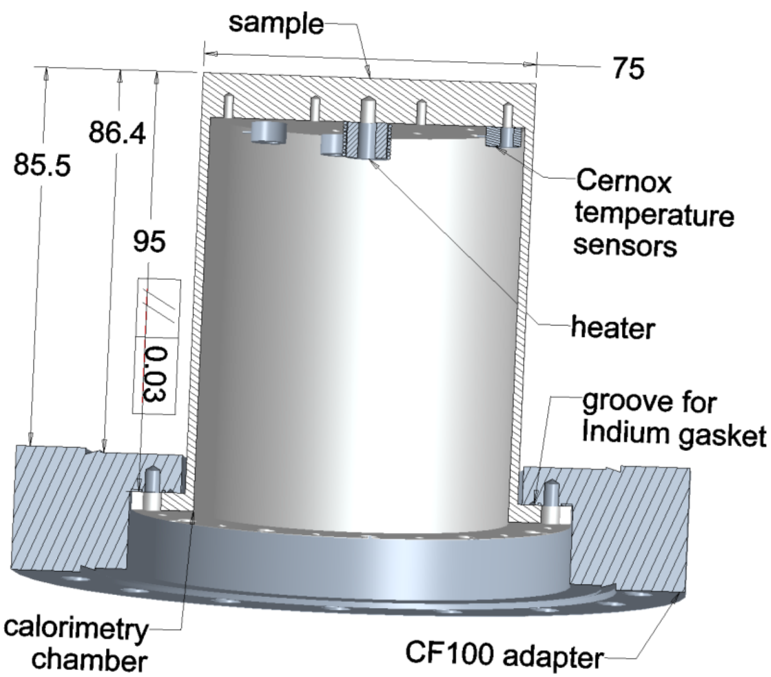
sample
75
86.4
85.5
95
0.03
Cernox
temperature
sensors
heater
groove for
Indium gasket
calorimetry
chamber
CF100 adapter

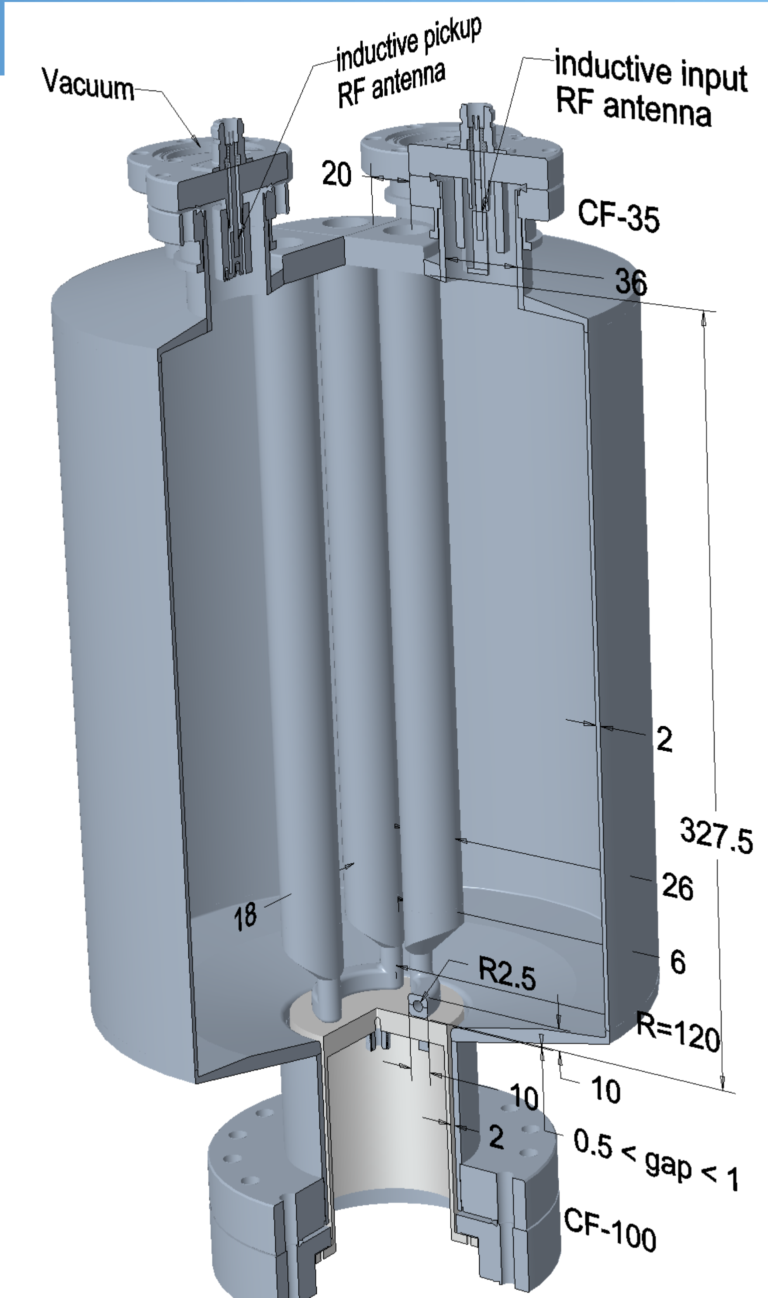
Vacuum
inductive pickup
RF antenna
inductive input
RF antenna
20
CF-35
36
2
327.5
26
6
18
R2.5
R=120
10
10
2
0.5 < gap < 1
CF-100

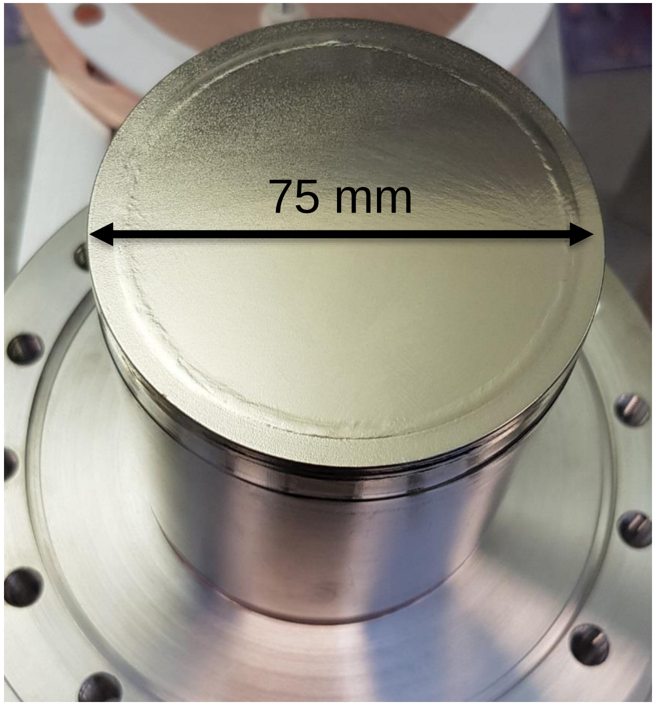
75 mm

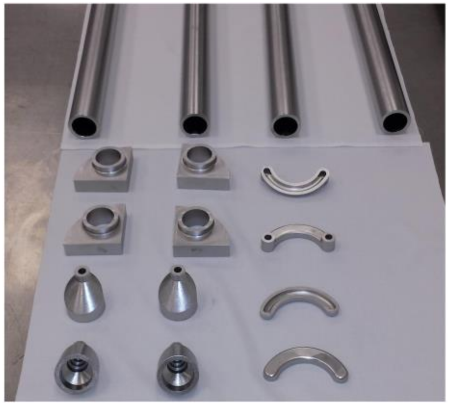

Fabricated from RRR 300 Niobium at Niowave Inc.

Buffered chemical polishing (BCP) at Jefferson Laboratory

High temperature bake (600°C)

High pressure rinse with ultra-pure water

Low temperature bake at 120°C for 48 hours

- Quadrupole modes near 415, 845, 1285 MHz
- Operated in vertical cryostat → LHe bath at 1.8 K
- Coaxial structure → thermal decoupling
- Calorimetric measurement of surface resistance
- $B_{Sample, max}$ ~ 120 mT (415 MHz) ~ 30 MV/m (TESLA)

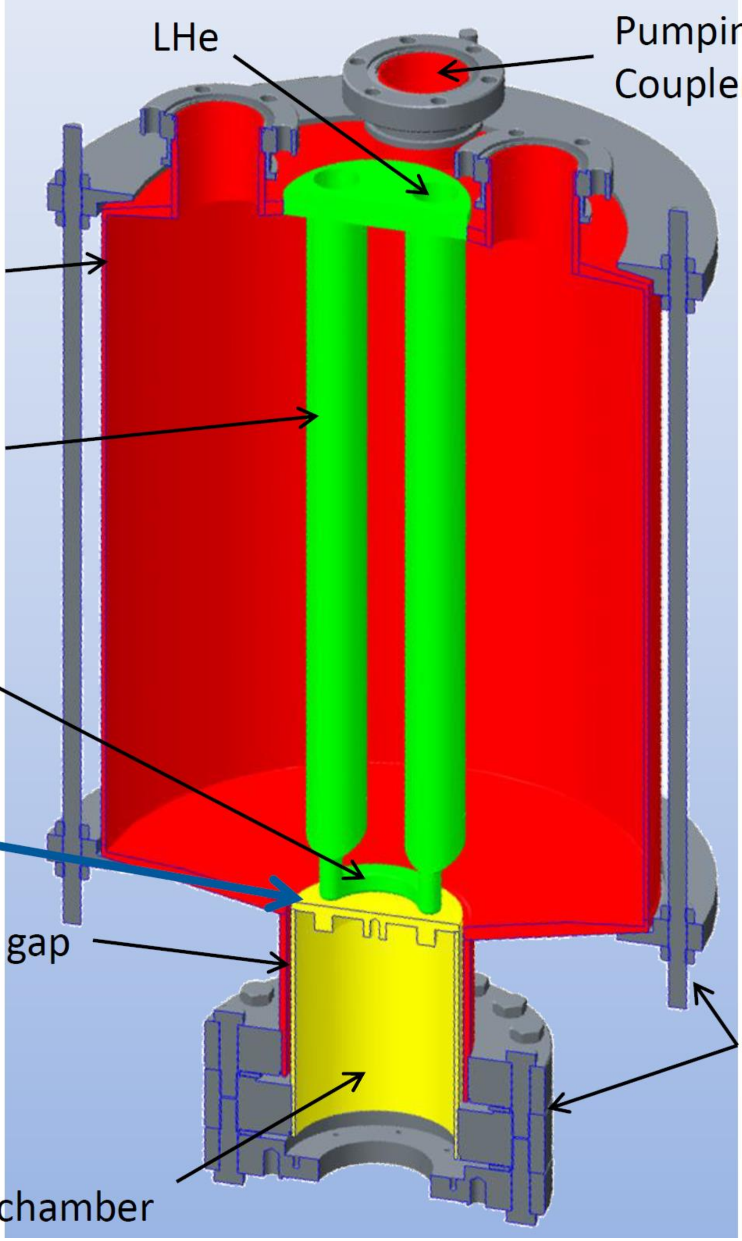

- Quadrupole modes near 415, 845, 1286 MHz
- LHe bath at 1.8 K
- Sample thermally decoupled from cavity <u>and</u> LHe bath
- $B_{\text{Sample, max}} \sim 120$ mT ~ 30 MV/m (TESLA)

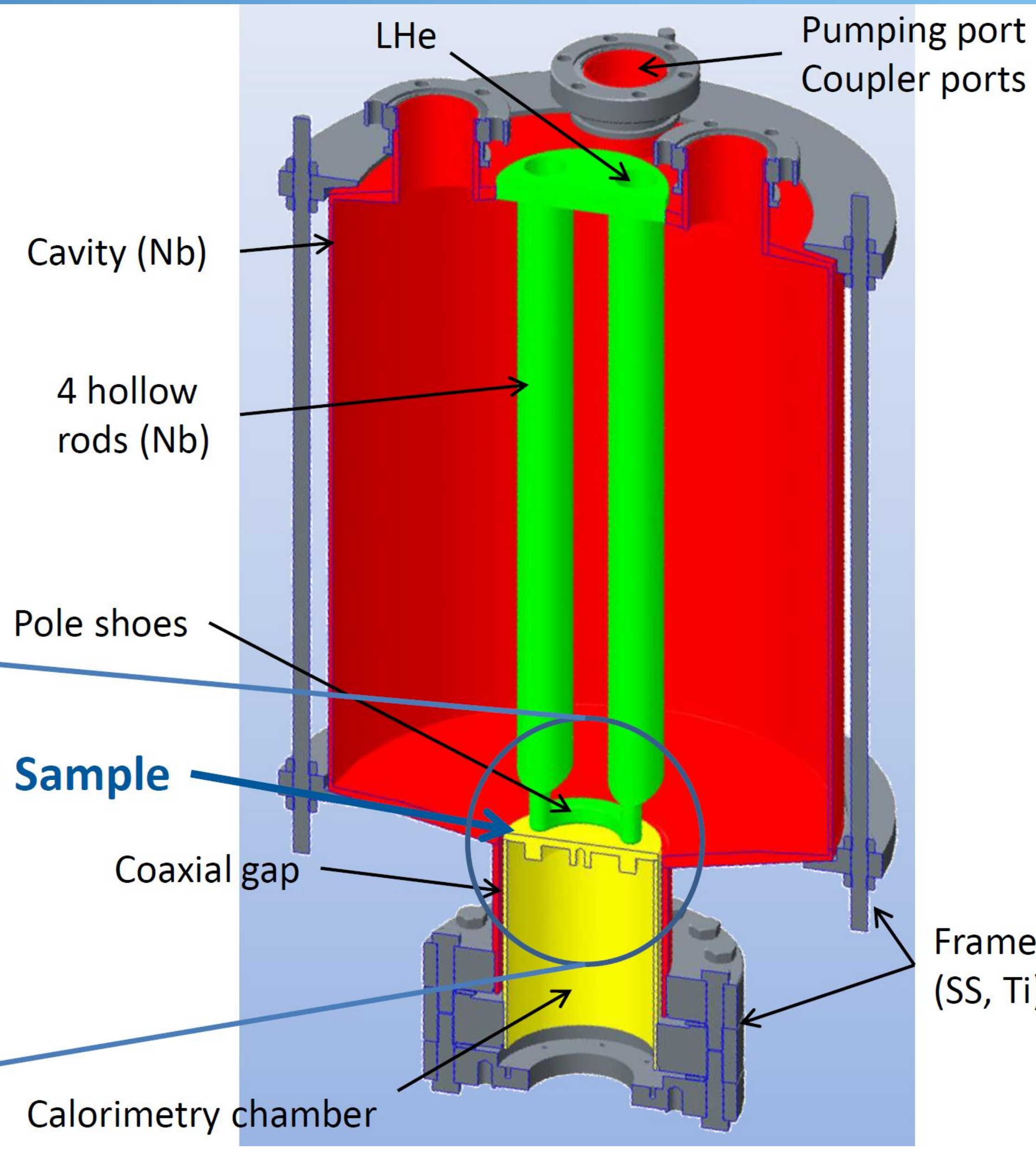

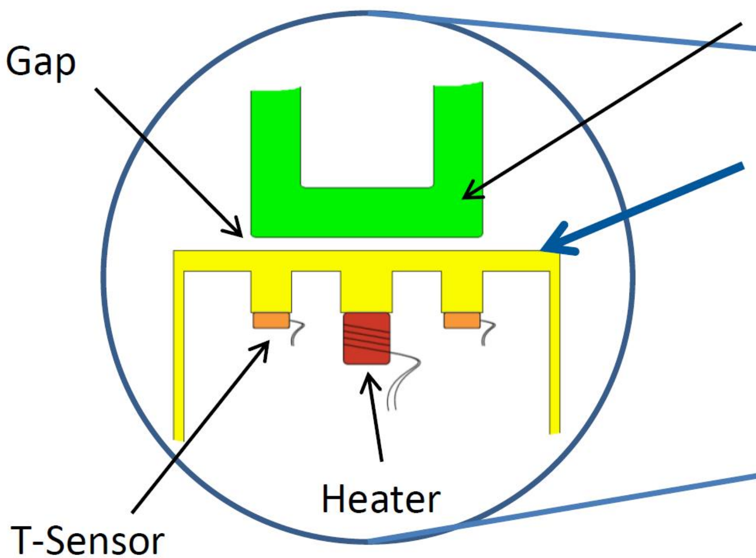

Accelerating cavity

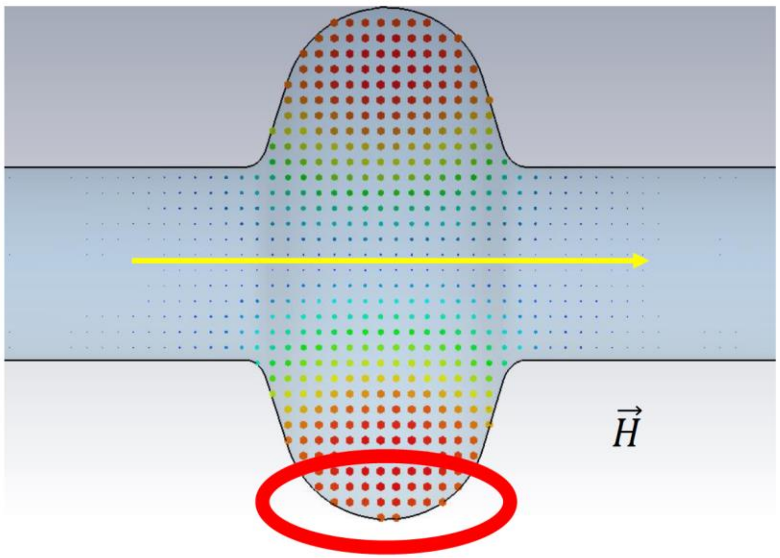

QPR

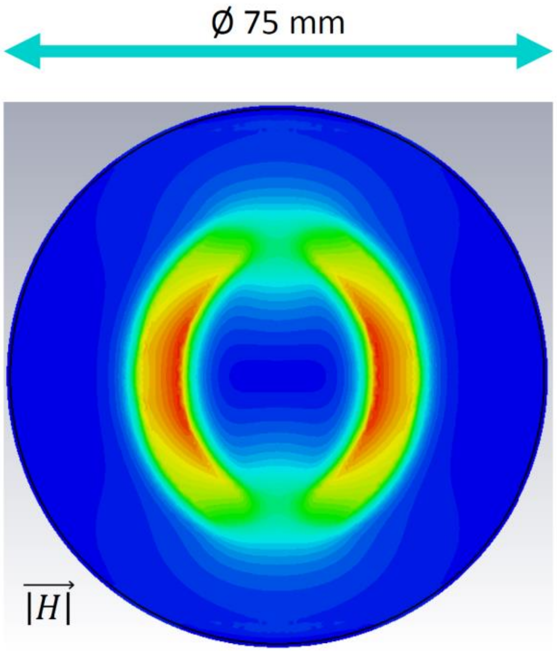

Focusing of E on axis, H on walls

Focusing of H on sample

courtesy Raphael Kleindienst

Frequency of drive system must be within bandwidth (20 Hz) around resonance frequency of cavity

- Pressure fluctuations in the helium and vibrational sources cause resonance frequency to shift (~400 Hz).

  Quadrupole Resonator very susceptible due to rod geometry.
- Feedback system necessary → phased-locked loop

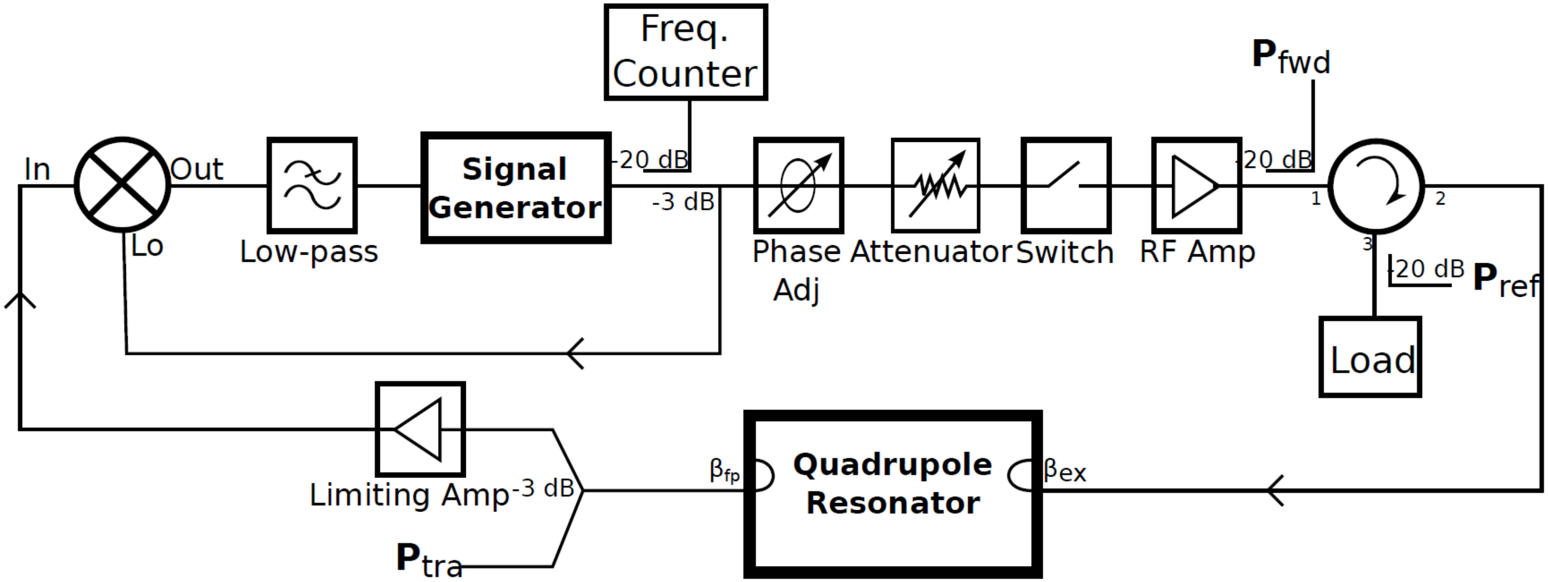

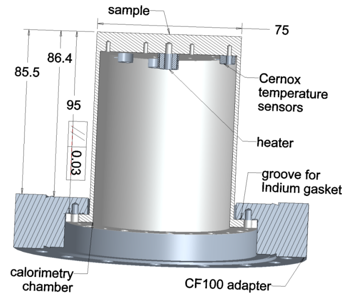

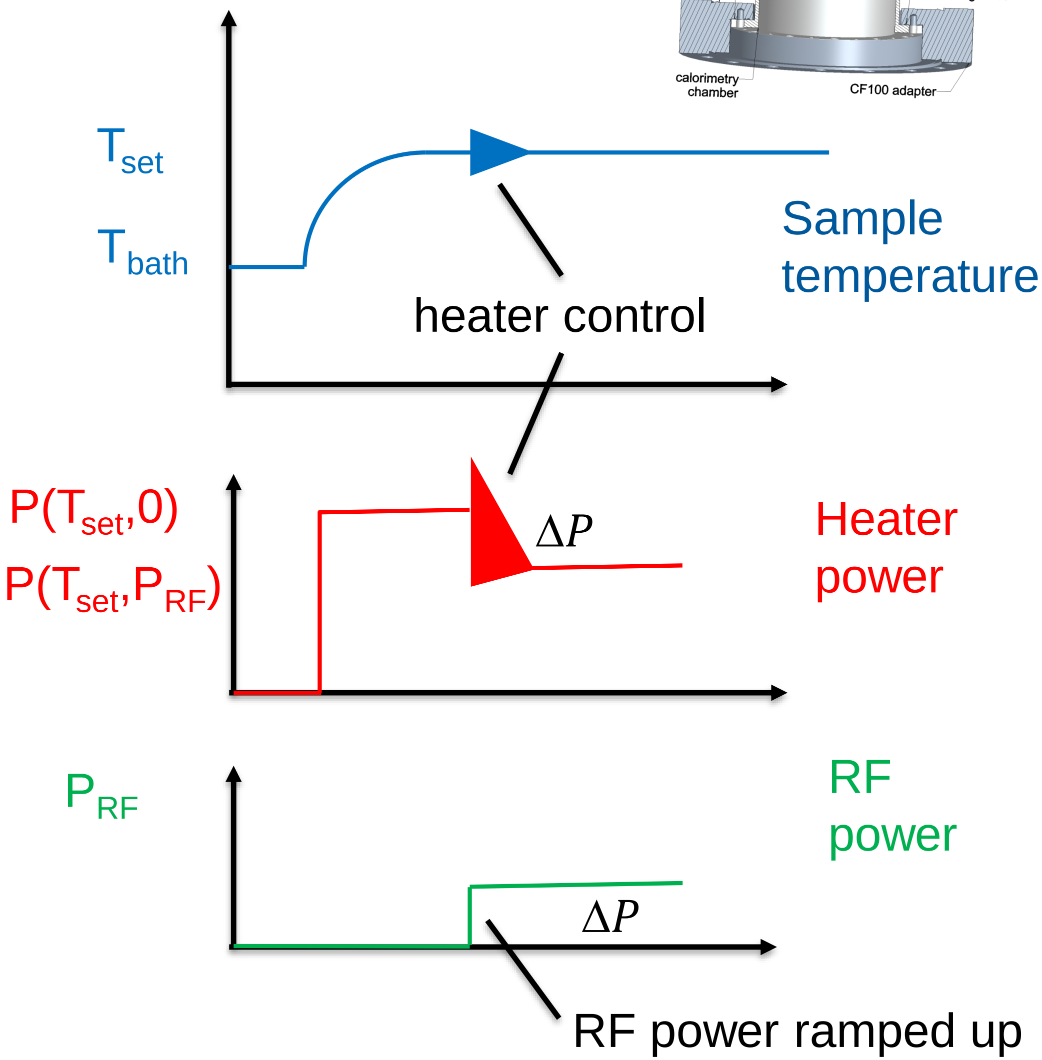

$$P_{RF} = P(T_{set},0) - P(T_{set},P_{RF})$$

$$= \frac{1}{2}\int_{smpl} R_s|H|^2 dS \approx R_s \frac{\omega U}{G}$$

geometry factor for sample

measured at heaters

$$R_s \approx \frac{G\Delta P}{\omega U}$$

frequency

stored energy, obtained from transmitted power measurement

$$B_{pk} = \frac{440\text{mT}}{\sqrt{1\text{J}}}\sqrt{U}$$

from numerical simulation

$$U = \frac{P_{transmitted} Q_{fp}}{\omega_0}$$

from measurement

Surface resistance

- $R_S(\omega, B_{RF}, T)$
- $R_{BCS} \leftrightarrow R_{res}$
- High resolution $R_S \approx 1\ \mathrm{n\Omega} \leftrightarrow Q_0 > 10^{11}$
- Cooling conditions
- Trapped flux

Penetration depth

- Penetration depth $\lambda(T)$
- Critical temperature T_c

RF quench field

- $B_{\mathrm{vp,\,RF}}(T, \omega)$
- T_c

- SC parameters: Energy gap Δ, Ginzburg-Landau parameter κ
- SC critical fields: H_{c1}, H_{sh}
- Electron mean free path ℓ, residual resistivity ratio (RRR)
- NC conductivity σ, skin depth δ

Characterization of two niobium samples at 416 MHz with different treatment treatment history:

	Sample A	Sample B
Structure	Large grain	Polycrystalline
Chemistry	150 $\mu\mathrm{m}BCP$	150 $\mu\mathrm{m}BCP$
HT bake	600 $^\circ$	600 $^\circ$
LT bake	120 $^\circ$, 48 hours	-

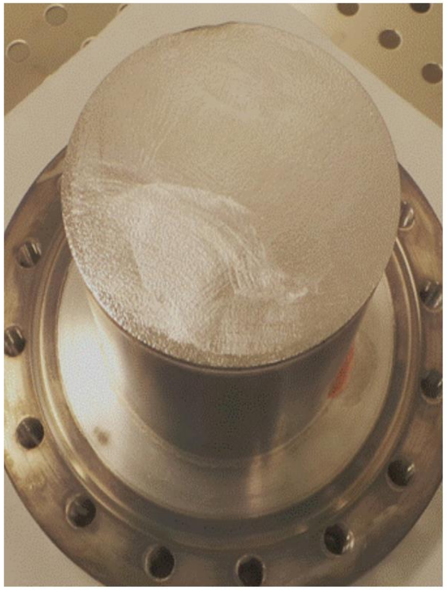

Sample A

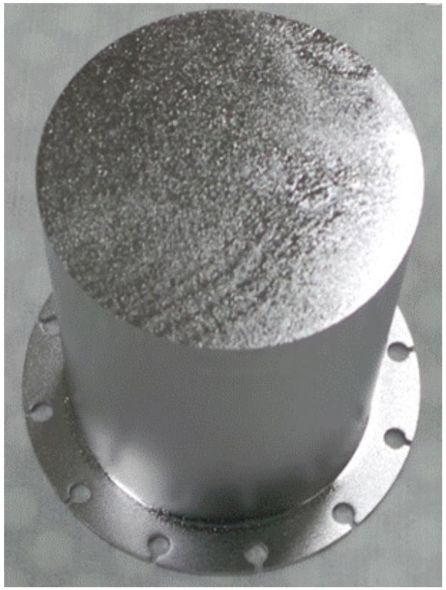

Sample B

courtesy Raphael Kleindienst

- Measurement at low RF field (20 mT)
- Arrhenius equation provide good fit to data for $T < T_C/2$

$$R_S(T) = A \cdot \frac{\omega^2}{T} \cdot \exp\left(-\frac{\Delta}{k_B T}\right) + R_{res}$$

- Reduced mean free path observed for Sample A as expected
- Unexpected large energy gap for Sample A (model-independent)

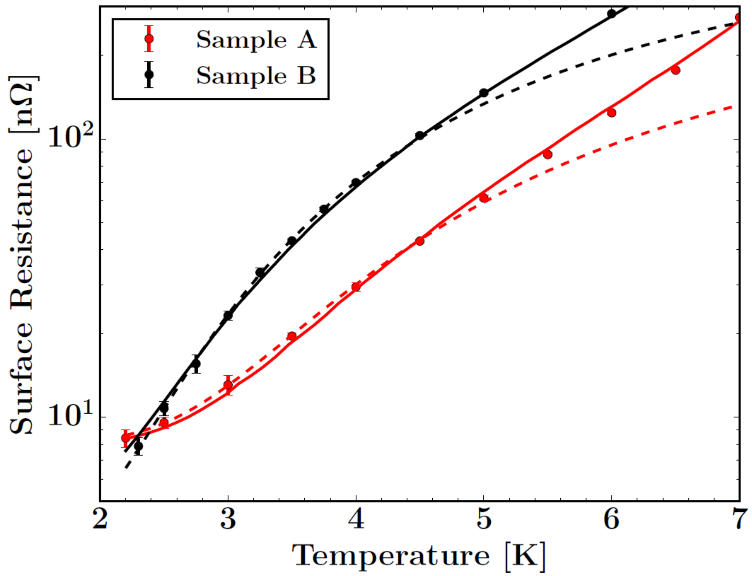

	Fit	$\Delta/k_B T_C$	R_{Res} [nΩ]	l [nm]	A [kΩ · Ks²]
Sample A	Arrhen.	$2.25^{+.069}_{-.022}$	$7.94^{+0.62}_{-0.81}$		$15.4^{+8.61}_{-5.44}$
120 °C bake	BCS	$2.18^{+.013}_{-.009}$	$8.98^{+0.65}_{-0.52}$	$14.5^{+3.10}_{-2.57}$	
Sample B	Arrhen.	$1.95^{+.082}_{-.016}$	$3.456^{+1.24}_{-1.49}$		$23.4^{+5.24}_{-5.87}$
	BCS	$1.778^{+.039}_{-.034}$	$4.53^{+1.31}_{-1.51}$	$24.33^{+14.82}_{-6.41}$	

- **Heat sample to temperature of interest**
- **Apply RF pulses of increasing amplitude until field break-down occurs**
- **Critical field follows T^2 dependency**
- **Measured field > literature value**
  we actually measure superheating field H_{sh}

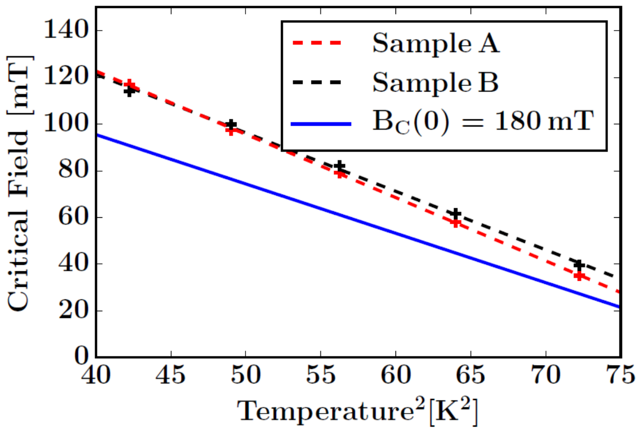

	Sample A	Sample B
$B_{C,RF}$	$(231 \pm 2.4)\,\mathrm{mT}$	$(221 \pm 3.7)\,\mathrm{mT}$
T_C	$(9.23 \pm 0.04)\,\mathrm{K}$	$(9.39 \pm 0.07)\,\mathrm{K}$

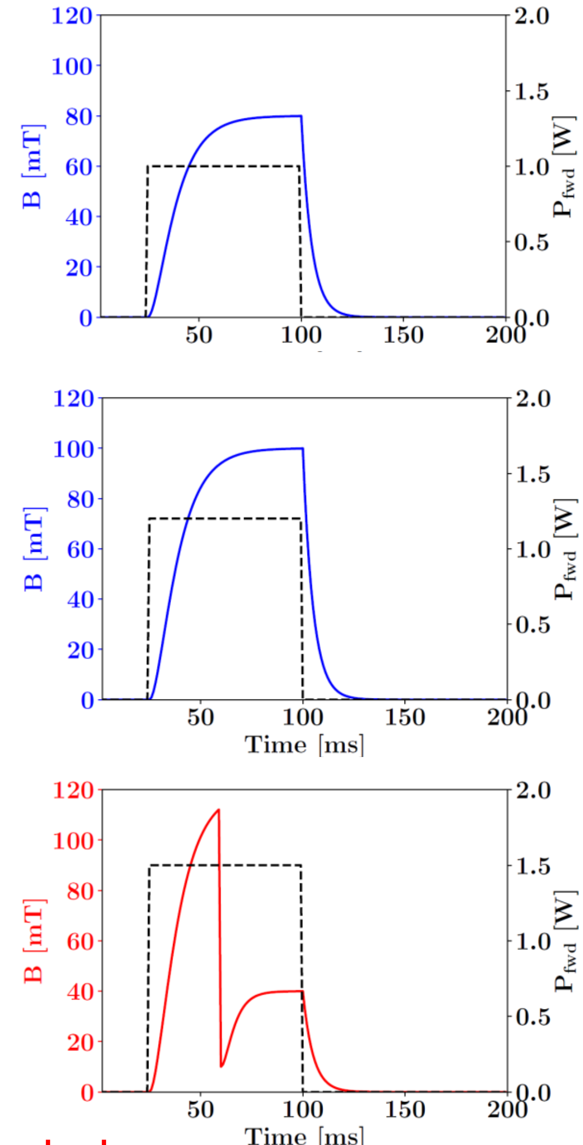

break-down

$$\lambda(T) = \frac{\lambda_0}{\sqrt{1 - \left(T/T_c\right)^4}}$$

temperature dependence of London penetration depth (Gorter-Casimir expression)

$$\frac{\Delta f}{f} = \frac{\Delta U}{U} = \frac{\int_{\delta V}(\epsilon_0 E^2 - \mu_0 H^2)dV}{\int_V (\epsilon_0 E^2 + \mu_0 H^2)dV}$$

Slater‘s theorem: frequency shift of resonant mode under small volume variation δV

$$G_{sample}(f) = \frac{2\pi f \mu_0 \int_V |H|^2 dV}{\int_S |H|^2 dS}$$

define sample geometry factor

$$\Delta f = \frac{-\pi\mu_0 f^2}{G_{sample}(f)} \Delta\lambda$$

$$\Delta\lambda = \lambda(T) - \lambda_0$$

apply to small volume between rods and sample, neglect E-fields, $\Delta V = \Delta\lambda \times S$ (S *is sample area*)
Δf easy to measure in SRF cavities (due to their small bandwidth)

$$\lambda(T) = \lambda_0 - \frac{G_{sample}(f)}{\pi\mu_0 f^2} \Delta f$$

measure (temperature dependence of) London depth with QPR courtesy Sebastian Keckert

S-I-S‘ multilayer sample

$$\Delta f = -\frac{\pi \mu_0 f^2}{G_{\mathrm{Sample}}(f)} \Delta\lambda_{\mathrm{eff}} \qquad \lambda_{\mathrm{eff}}(T) = \frac{1}{B_0}\int_0^\infty B(x,T)\,\mathrm{dx}$$

(B(x,T) from multilayer theory)

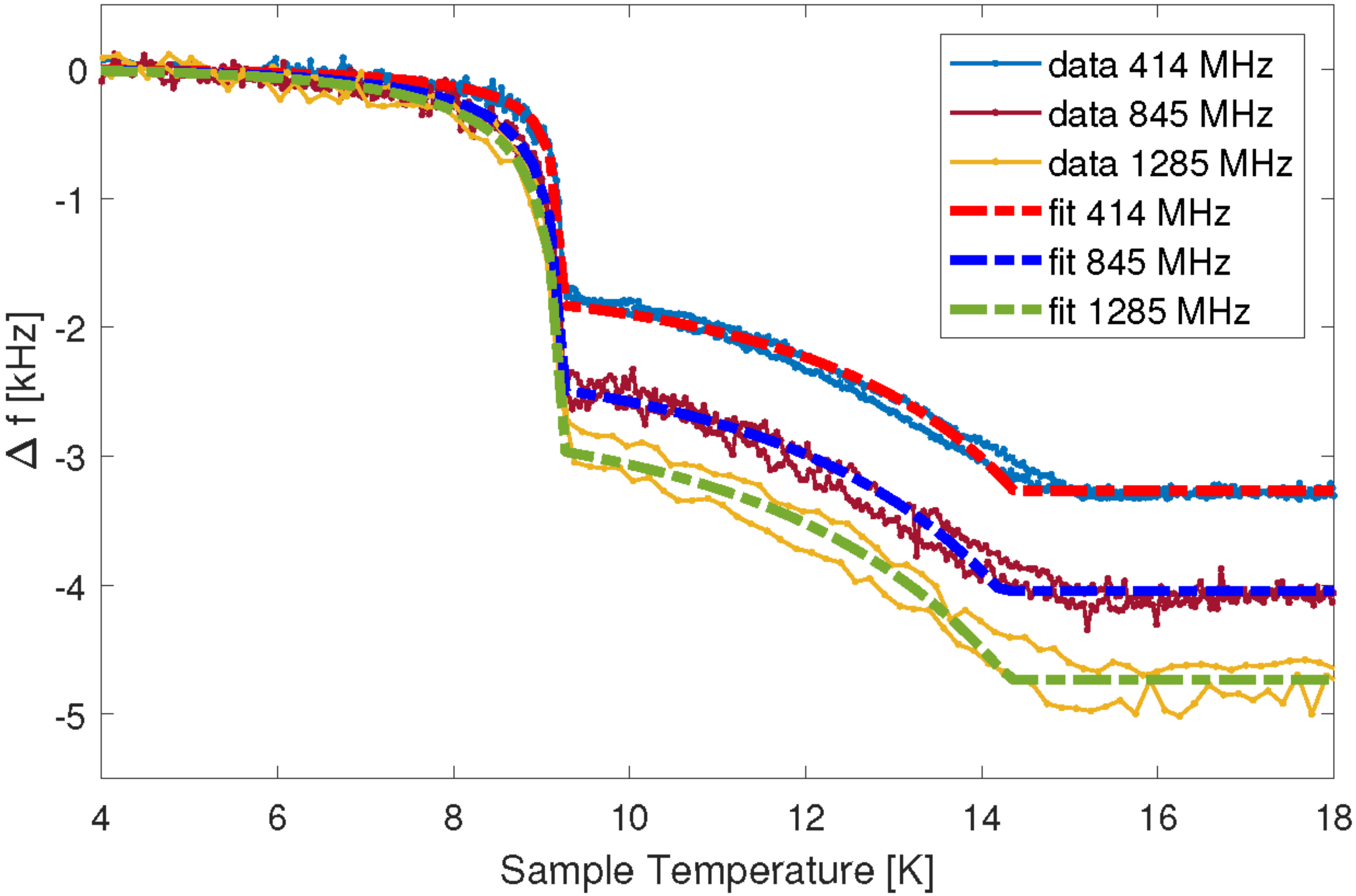

courtesy Raphael Kleindienst

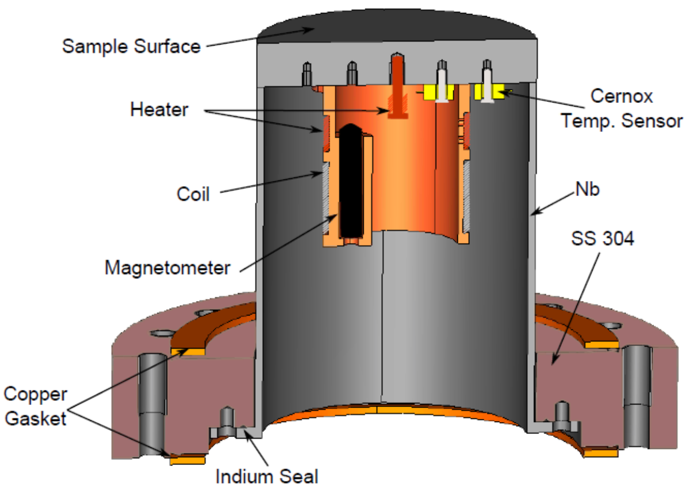

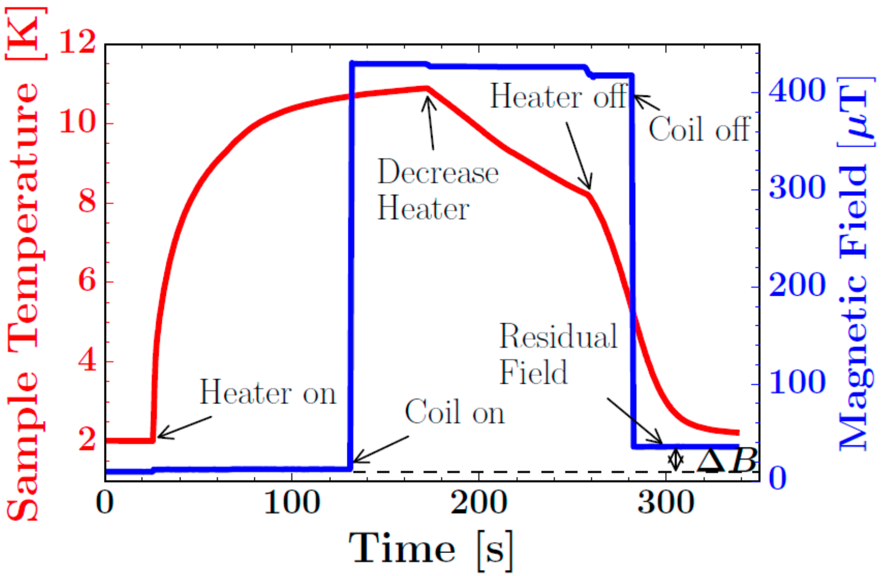

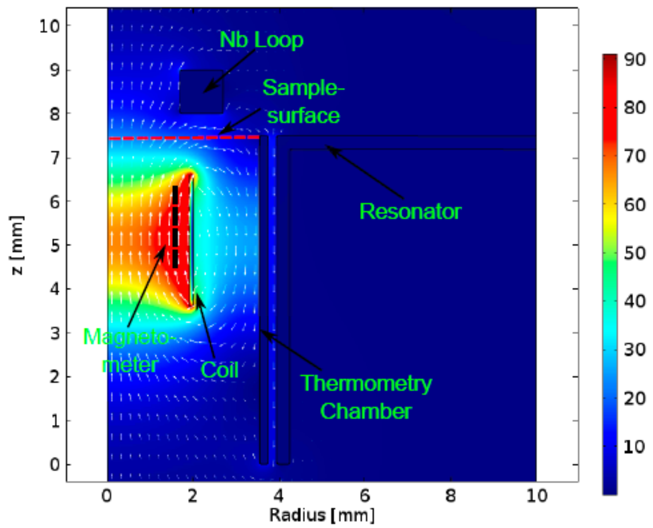

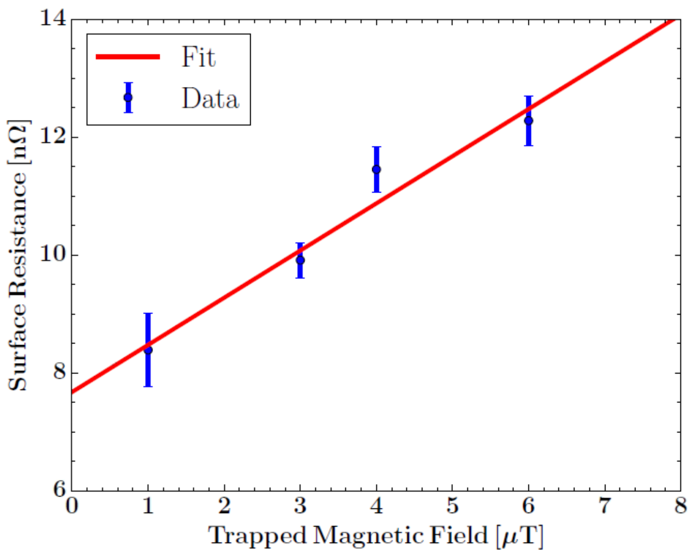

OTHER RF TESTING DEVICES

Parallel Plate Resonator

- Moderate sensitivity
- High frequency
- Very convenient

Taber RSI 1990

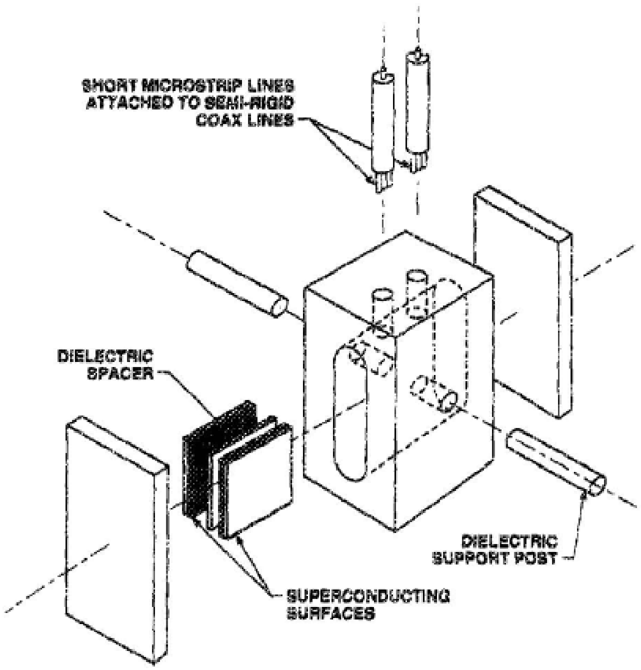

FIG. 1. Expanded view of the measurement configuration. The material under test is clamped within the test chamber by two dielectric posts that are spring loaded by components (not shown) exterior to the test chamber.

f (GHz)	A_{Sample}	A_{rf}	$R_{sens}(\Omega)$	B_{max} (mT)
10	1 cm^2	1 cm^2	1e-5	?

TE_{011} cavity with flat samples

- Large sample plate
- 100 sensitive thermometers

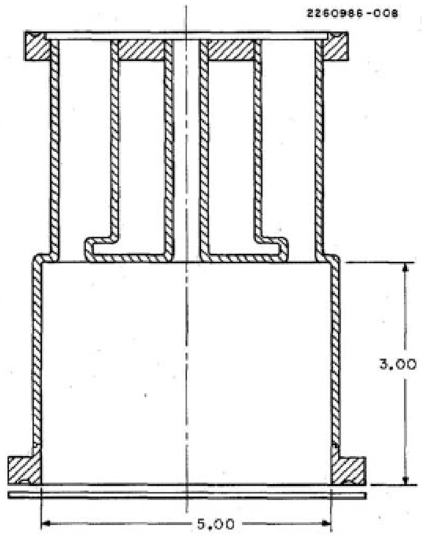

Figure 4. Cross-section of TE_{011} cavity (dimensions in inches).

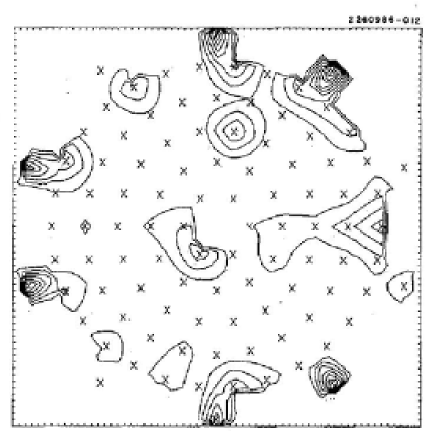

Figure 8c. "Residual Resistance" Contour map - logarithmic scale.

Kneisel et al. ASC 1986 (MAG-23 1987)

f (GHz)	A_{Sample}	A_{rf}	$R_{sens}(\Omega)$	B_{max}
3.5	127 cm^2	127 cm^2	1 e-9	2 mT

“Mushroom” Cavity

- Probe H_{max} with pulsed rf

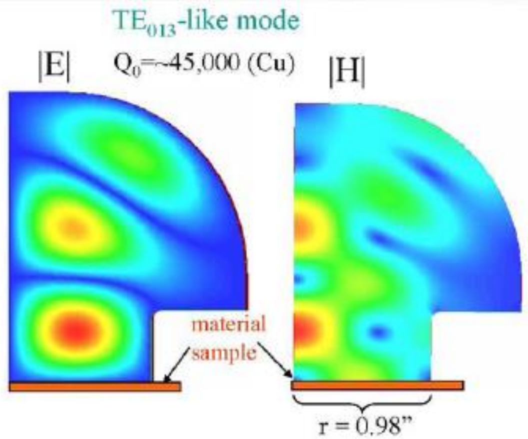

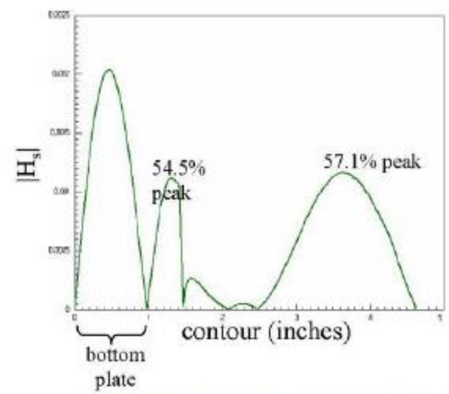

Nantista SLAC PAC 2005

- Superconducting materials test cavity
  - No surface electric fields (no multipacting)
  - Magnetic field concentrated on bottom (sample) face
- X-band (~11.424 GHz):
  - high power available
  - fits in cryogenic Dewar
  - Relatively large (2-3”) samples required

f (GHz)	A_{Sample}	A_{rf}	$R_{sens}(\Omega)$	B_{max}
11.4	19.6 cm^2	~8 cm^2	?	?

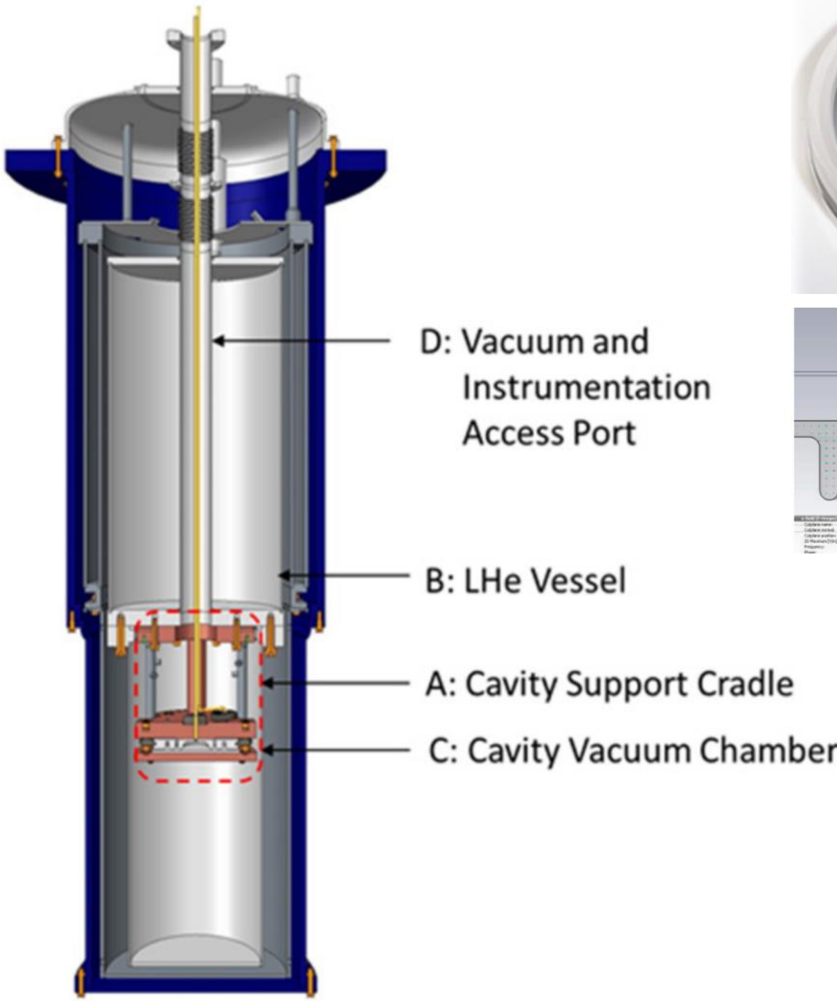

8 GHz choked cavity with concentric input coupler

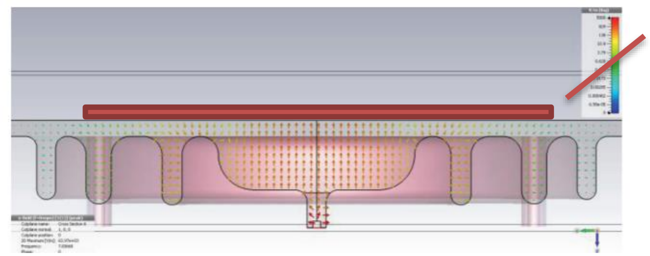

sample

E-field map

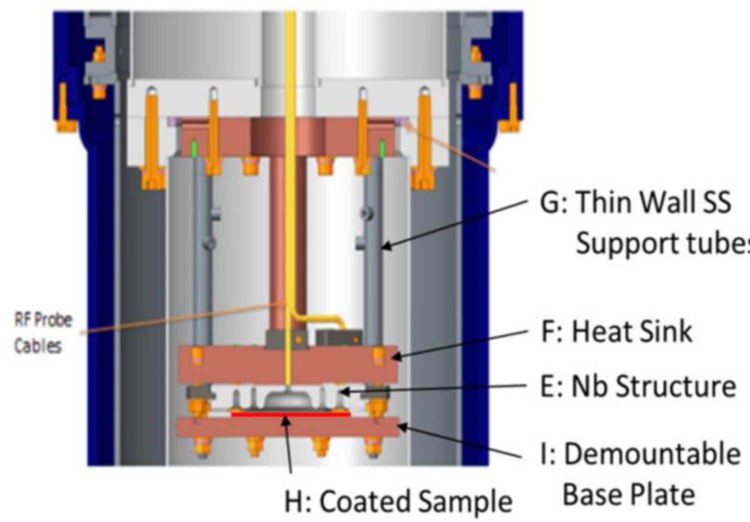

Goudket et al.

STRIPLINE RESONATOR

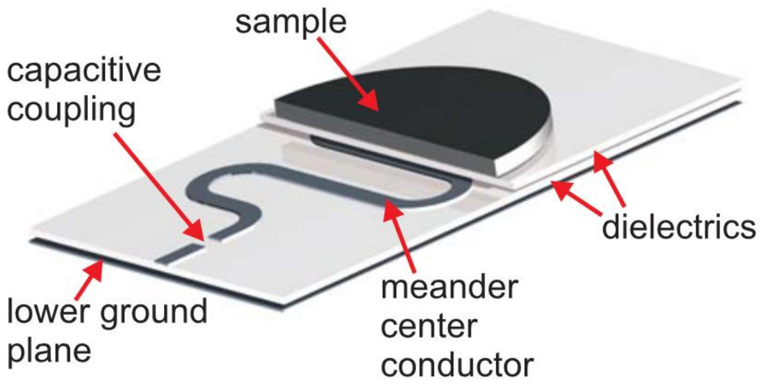

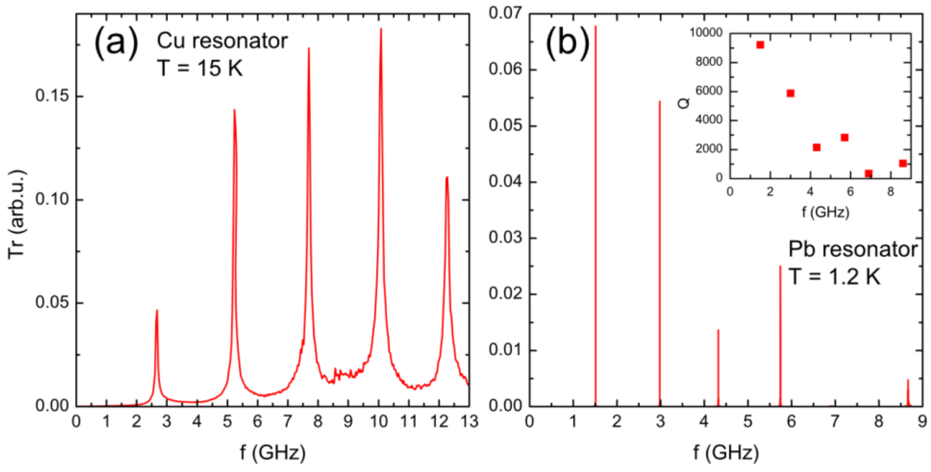

RF transmission spectra (S21)

Oates, et al., Scheffler et al.

Measurements on MgB_2

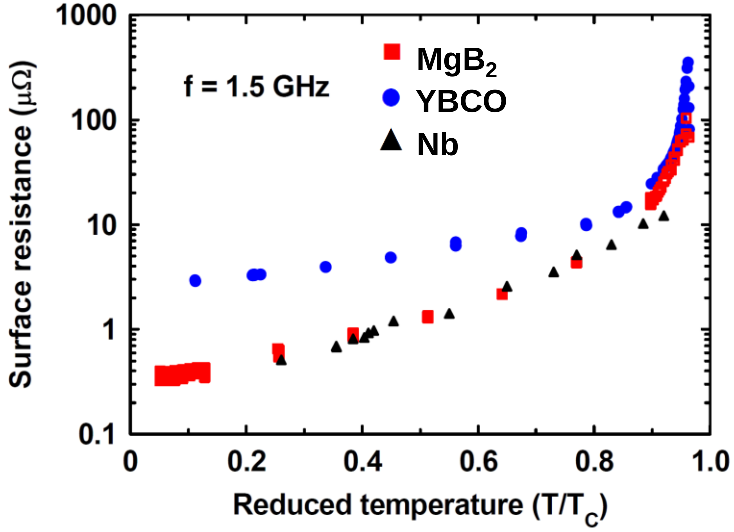

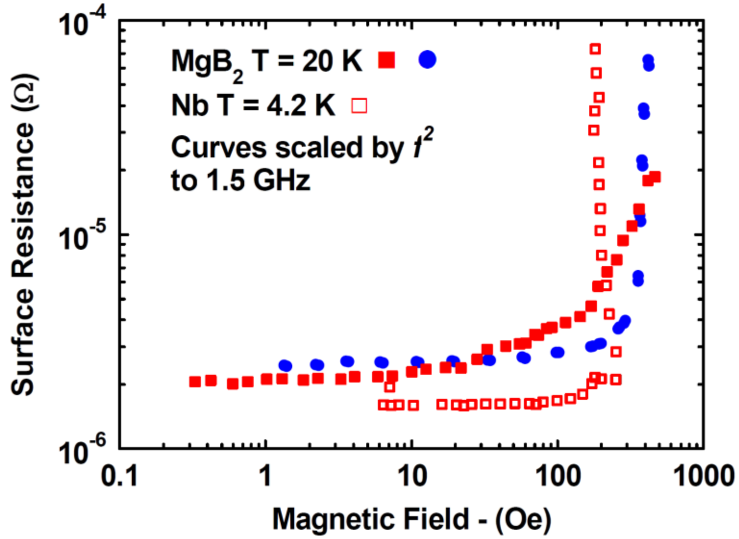

Moeckly et al.

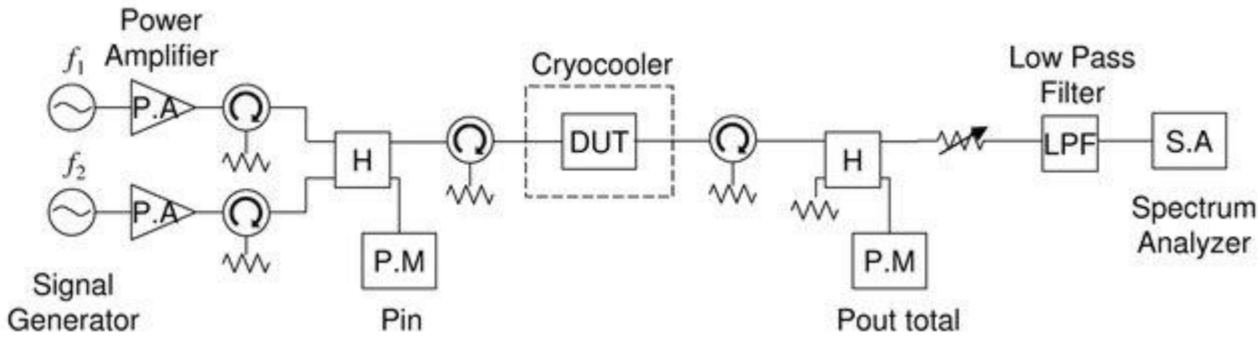

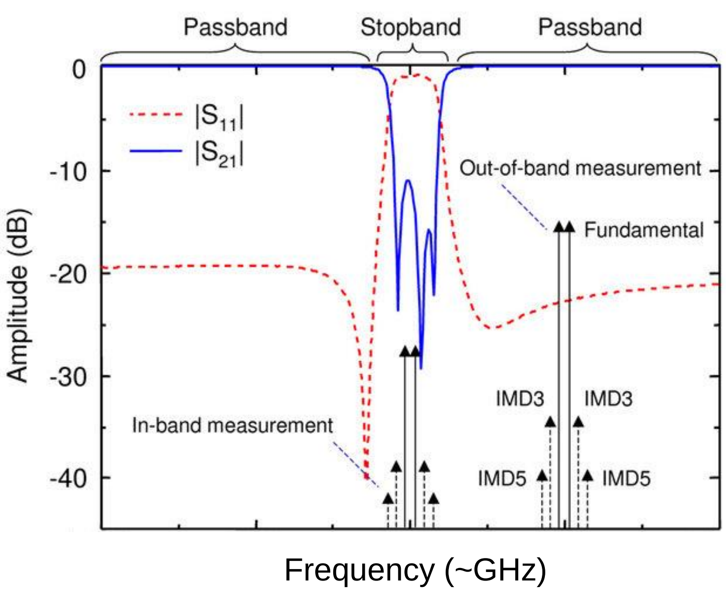

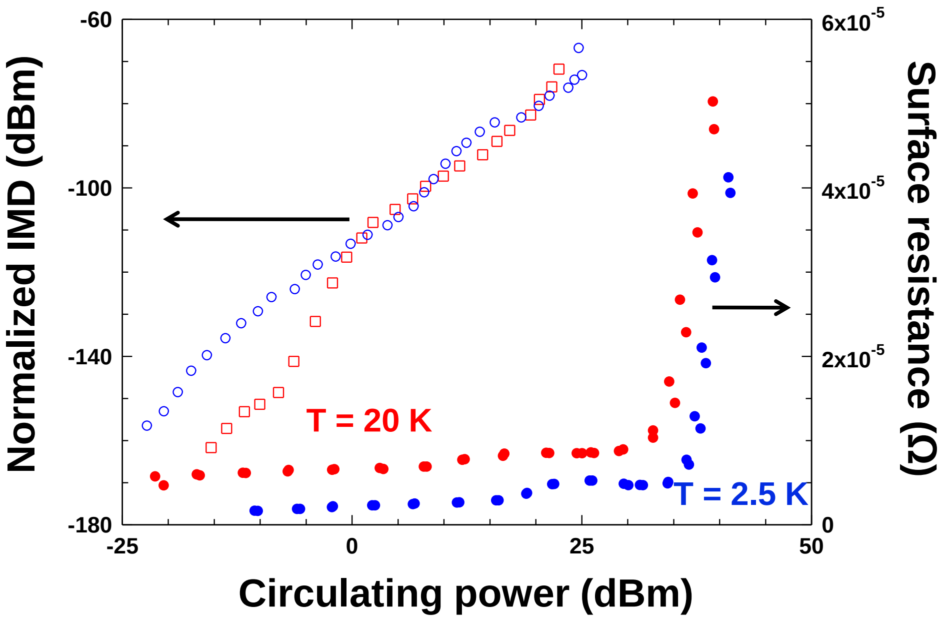

D. E. Oates, Y. D. Agassi, B. H. Moeckly,
IEEE TRANSACTIONS ON APPLIED SUPERCONDUCTIVITY, VOL. 17, NO. 2, JUNE 2007

Use IMD to detect non-linearities in superconducting properties

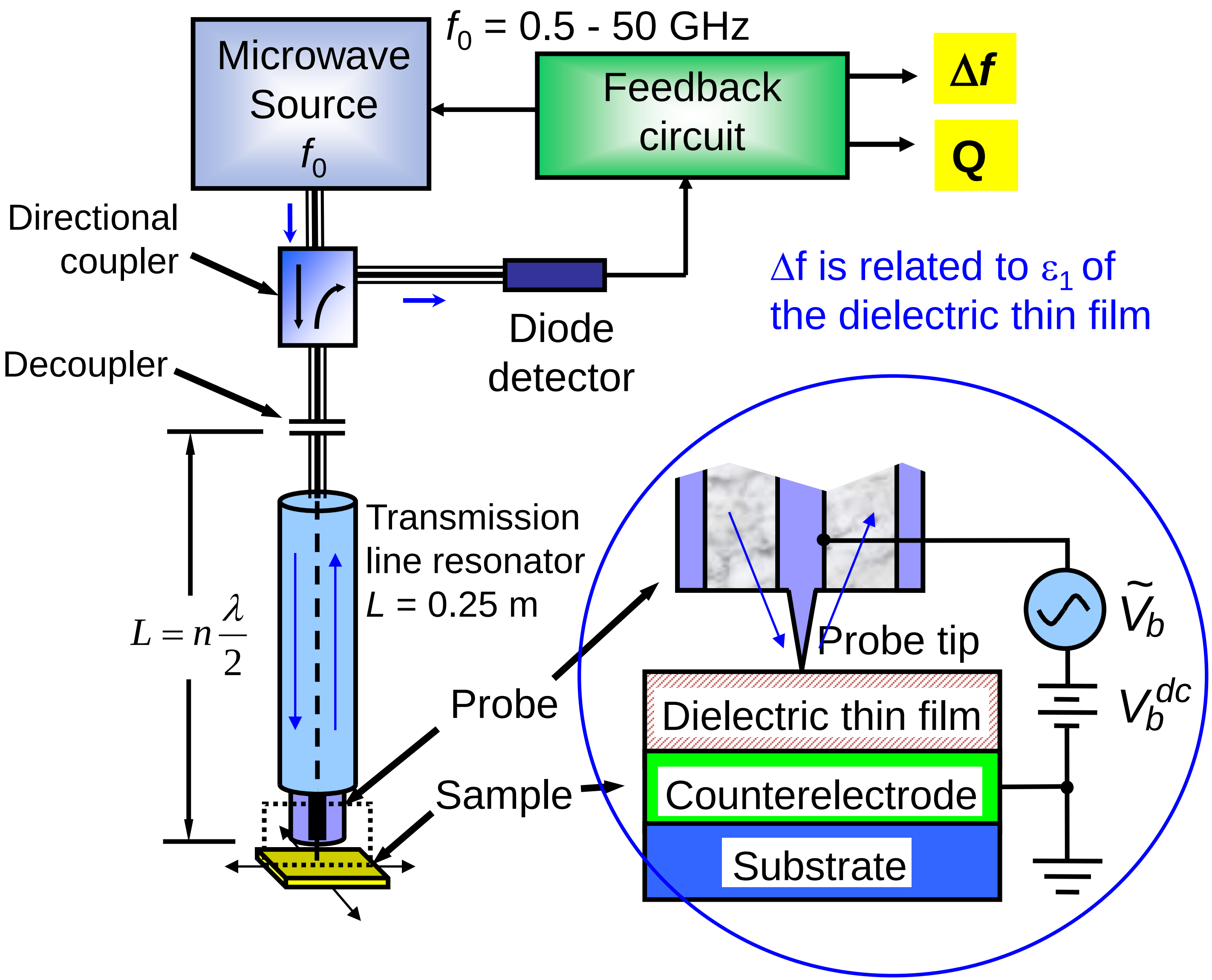

D. E. Steinhauer, *et al.*, Rev. Sci. Instrum. 71, 2751-2758 (2000)

1) Examine coupons with intense, localized B_{RF} in the superconducting state
2) Measure locally-produced harmonic generation from defects
3) Scan the probe and image the response

T. Tai, *et al*.
IEEE Trans. Appl. Supercond.
21, 2615 (2011); 23, 7100104 (2013)

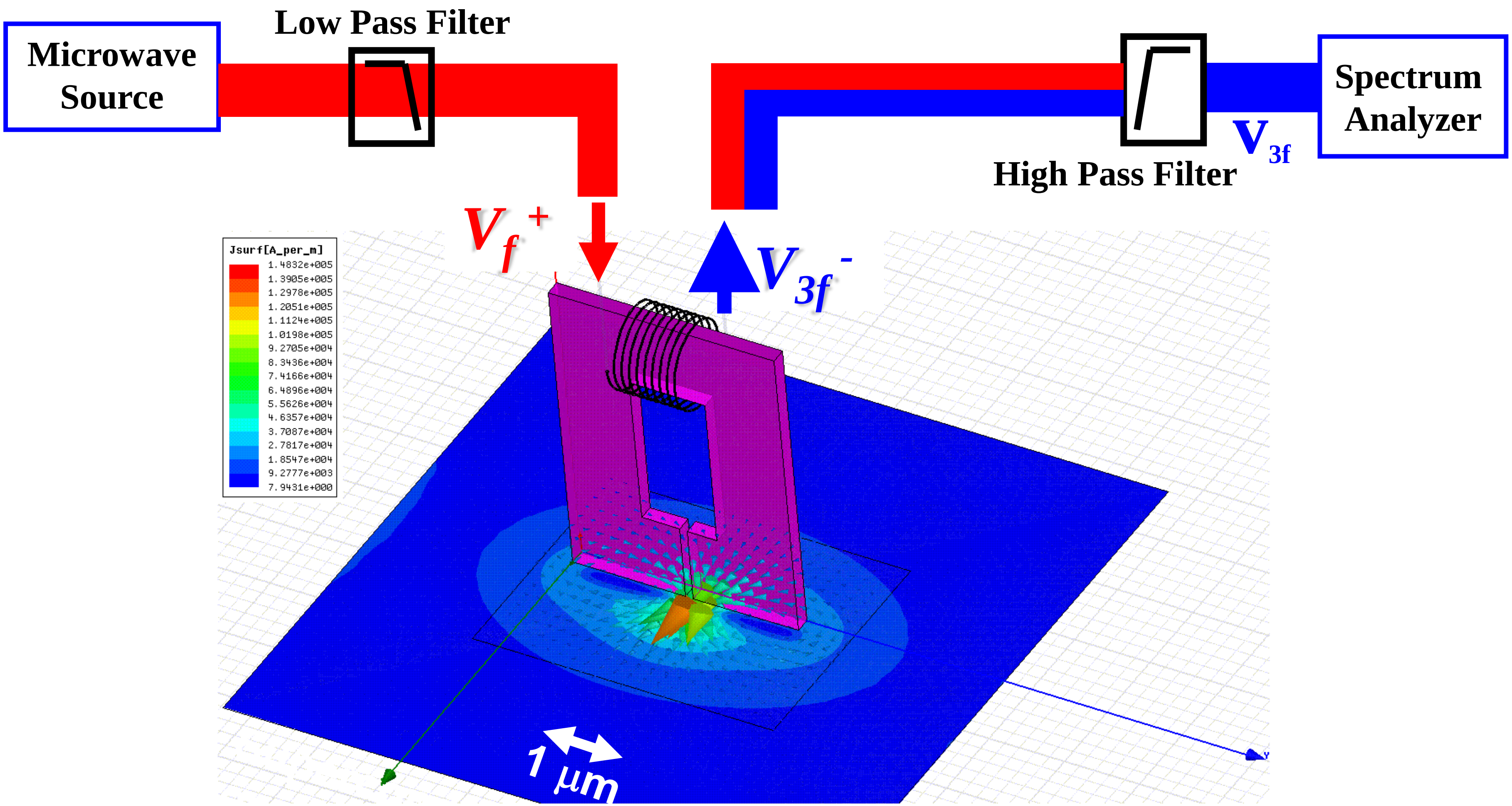

Courtesy Steven Anlage

Objective: Identify microscopic defects that cause breakdown of SRF cavities

Why harmonics?

IMD spectra exhibit features hidden to Rs measurements

Each defect type will have different nonlinear signature

Superconductor is the main source of Nonlinearity

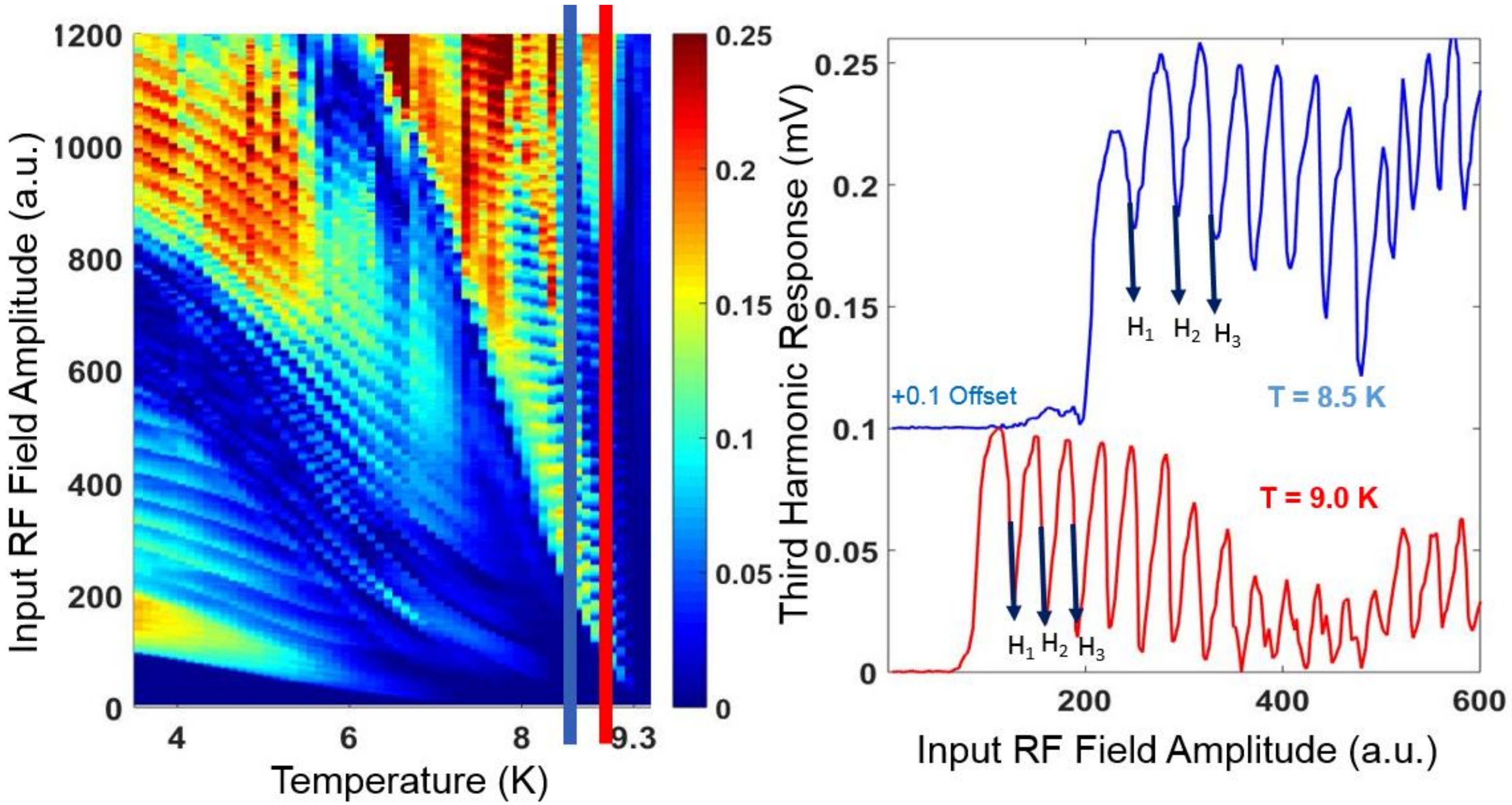

f=4.38 GHz

Courtesy Steven Anlage

Current Driven Resistively and Capacitively Shunted Josephson Junctions (RCSJ) model

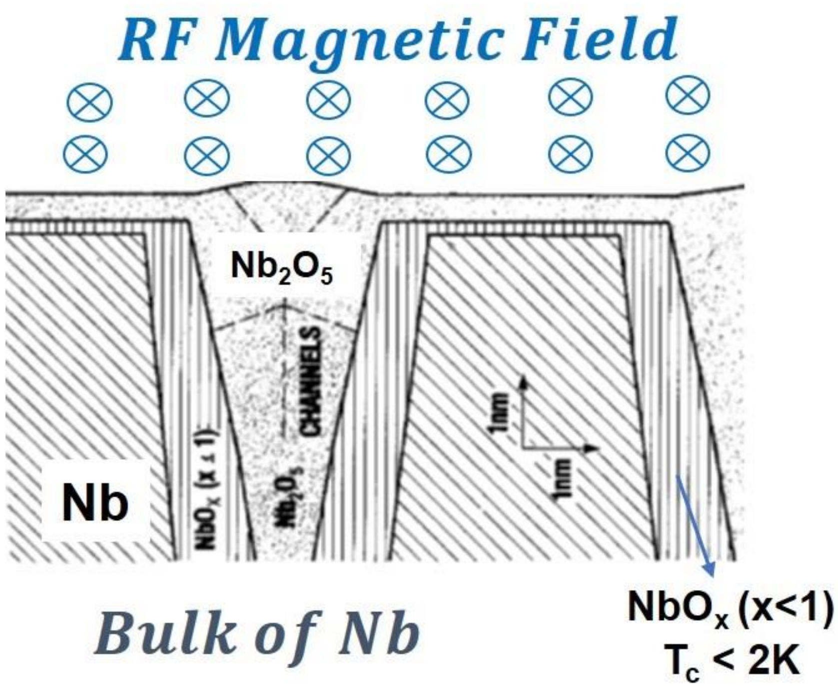

J. Halbritter, " **On the Oxidation and on the Superconductivity of Niobium,"** J. Appl. Phys. A 43, 1 (1987).

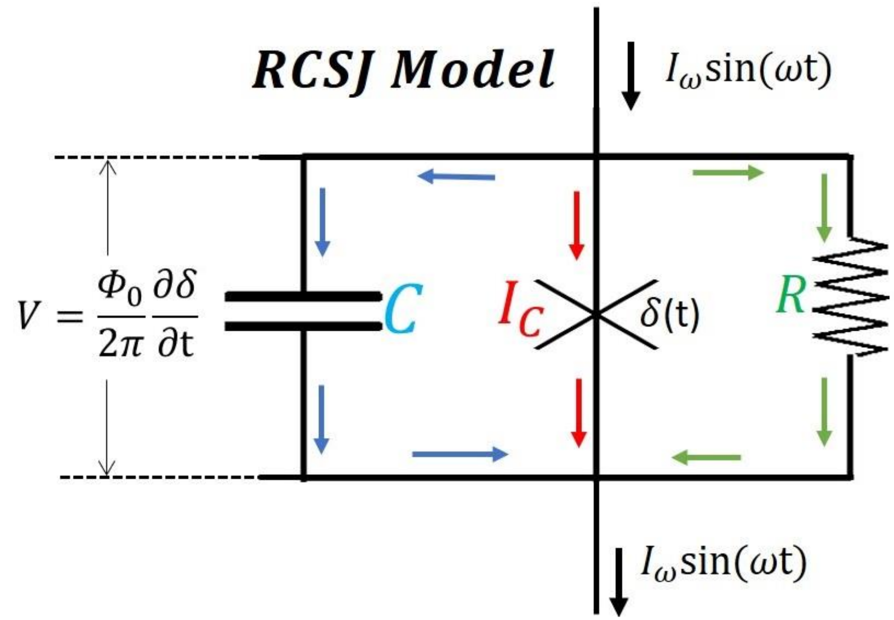

$$\frac{\Phi_0 C}{2\pi}\frac{\partial^2\delta}{\partial t^2} + I_C \sin\delta + \frac{\Phi_0}{2\pi R_n}\frac{\partial\delta}{\partial t} = I_\omega \sin(\omega t)$$

L. M. Xie, J. Wosik, and J. C. Wolfe, " **Nonlinear microwave absorption in weak-link Josephson junctions,"** Phys. Rev. B 54, 15494 (1996).

J. McDonald and John R. Clem, " **Microwave response and surface impedance of weak links,"** Phys. Rev. B 56, 14723 (1997).

Courtesy Steven Anlage

Solution to the RCSJ Model

$$\cancel{\frac{\Phi_0 C}{2\pi}\frac{\partial^2\delta}{\partial t^2}} + I_C sin\delta + \frac{\Phi_0}{2\pi R_n}\frac{\partial\delta}{\partial t} = I_\omega \sin(\omega t)$$

Short Junction Approximation

All Dimensions Perpendicular to the field << λ_J

$$(I_C R_n) sin\delta + \frac{\Phi_0}{2\pi}\frac{\partial\delta}{\partial t} = (I_\omega R_n)\sin(\omega t)$$

$\boldsymbol{I_C R_n}$ - Fitting Parameter

$\boldsymbol{I_\omega R_n}$- ScalingFactor * Input RF Field Amplitude (a.u.)

$\boldsymbol{\delta(t) \rightarrow V(t) \rightarrow V_{3\omega}}$

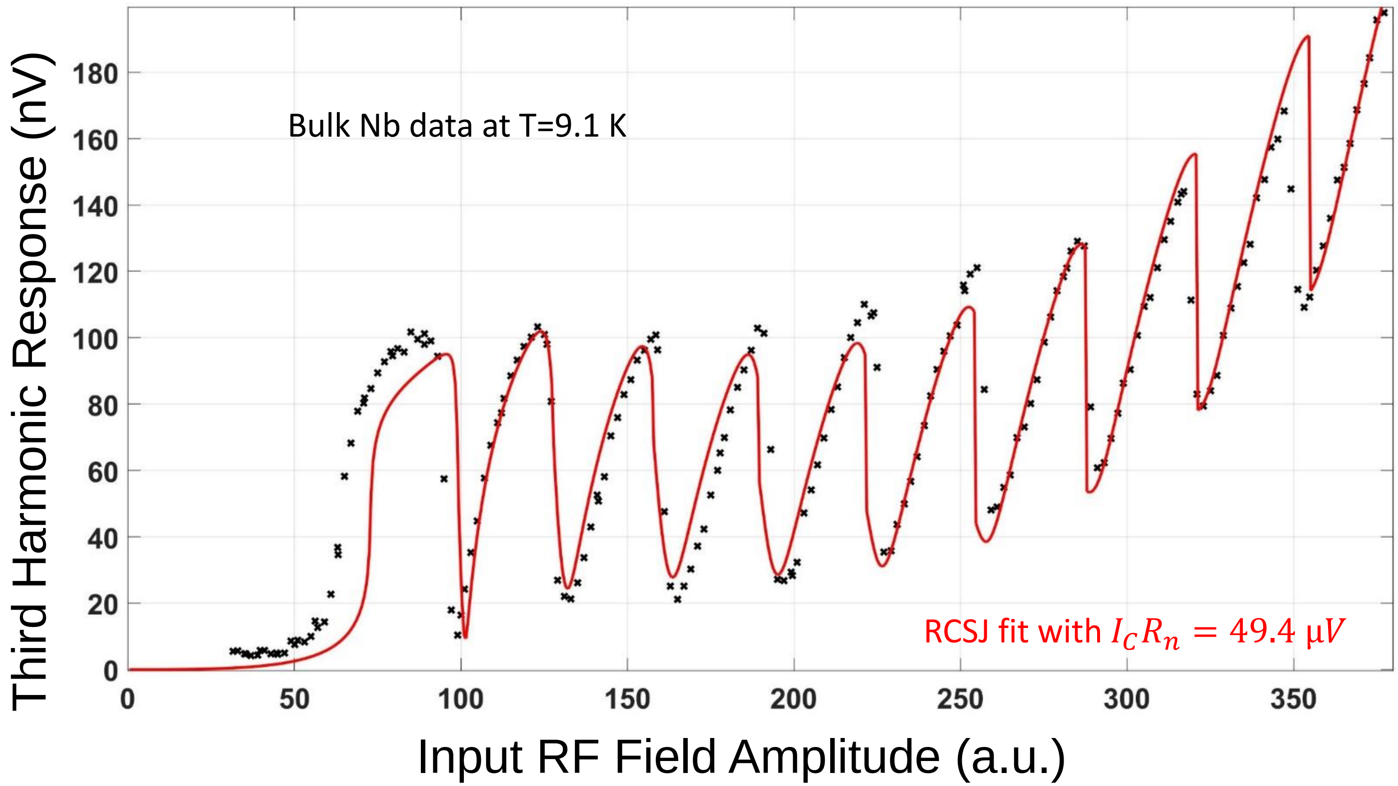

Courtesy Steven Anlage

DC TECHNIQUES (also low frequency techniques)

You learn a lot from these techniques, **BUT:**
for SRF applications you need to measure at or near your operating frequency

consider these methods an intermediate step

$$I_{ac}(t) = I_0\omega\cos\varpi t$$ ac current for primary coil

$$V_B(t) = (M_1 - M_2)\frac{dI_{ac}}{dt} = -(M_1 - M_2)I_0\omega\sin\varpi t$$

Background voltage (without sample)

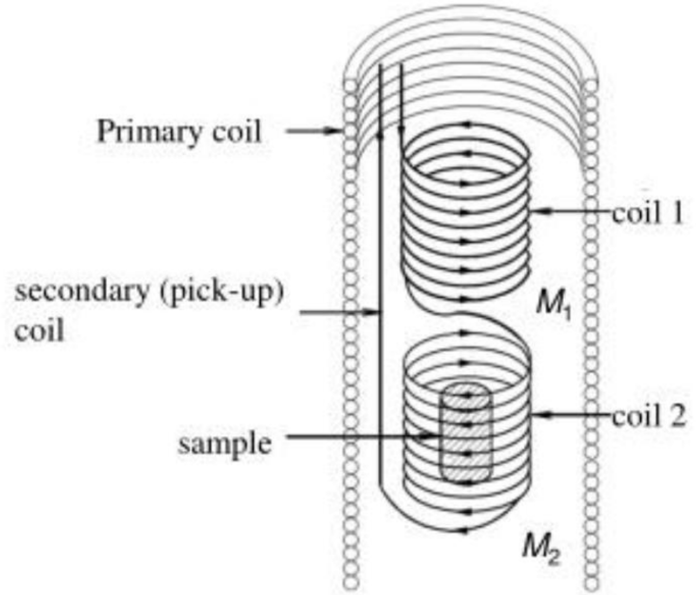

$$V_1(t) = V_B(t) + V_{s1}(t)$$ Sample in coil 1

$$V_2(t) = V_B(t) - V_{s2}(t)$$ Sample in coil 2

$$\boxed{V_{s1}(t) = -N_1 S_1 f\chi_{ac}\frac{dh_{ac}(t)}{dt}}$$

N: # of turns
S: cross section area
f: filling factor
h_{ac}: oscillating external field
χ_{ac}: complex susceptibility (χ'-i χ'')
χ': in-phase signal
χ'': out of phase signal

$M_{1,2}$: mutual inductance between primary and secondary

$$\boxed{V_{1,rms} - V_{2,rms} = V_{s1,rms} + V_{s1,rms} = \{(N_1S_1 + N_2S_2)f\varpi\}\, h_0\chi_{ac} = \frac{h_0\chi_{ac}}{C_\chi}}$$

$$C_\chi = \frac{1}{(N_1S_1 + N_2S_2)f\varpi}$$ calibration factor (sensitivity)

D. Gokhfeld, Journal of Siberian Federal University. Mathematics & Physics 2018, 11(2), 219–22

trapped flux

virgin curve M(H)=-xH for $H<H_{c1}$, x determined by demagnetization factor and fraction of sc phase

irreversibility field: M(H) becomes reversible at $H> H_{irr}$

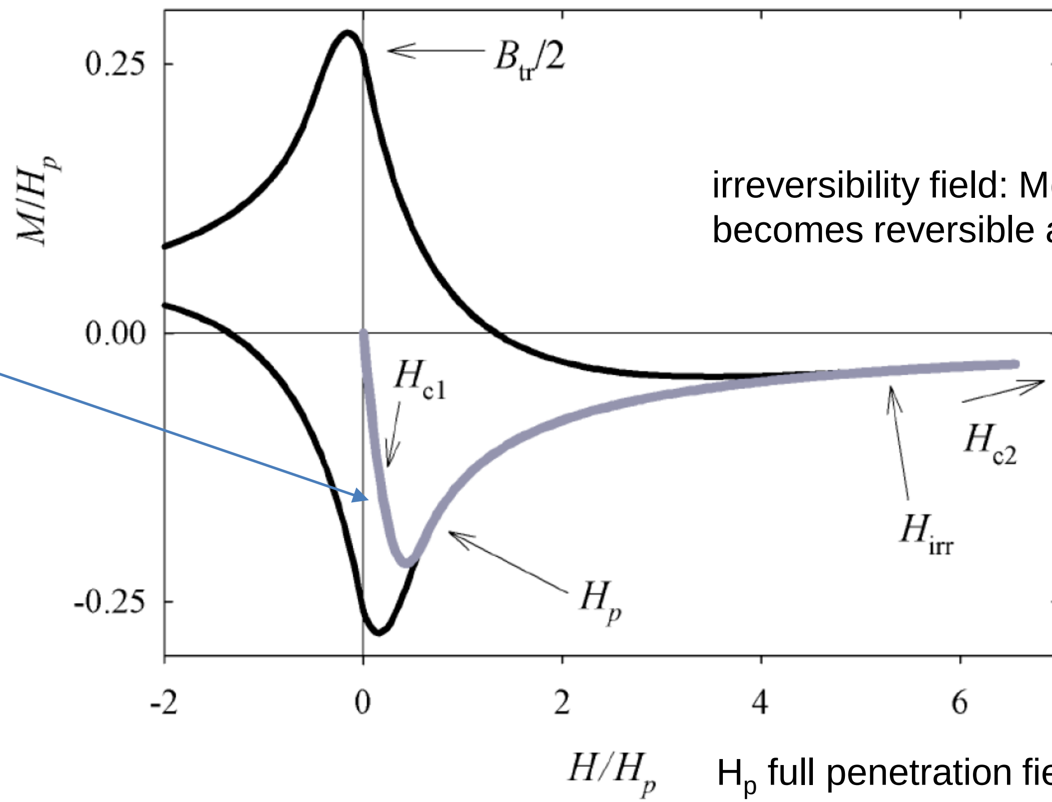

H_p full penetration field where virgin curve coincides with loop courtesy Claassen, Lamura, Antoine

Method to measure onset of flux penetration at H_{c1}

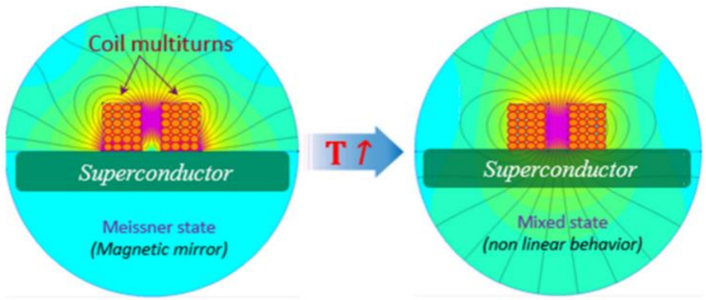

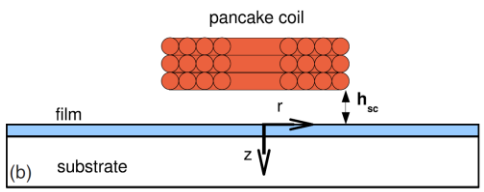

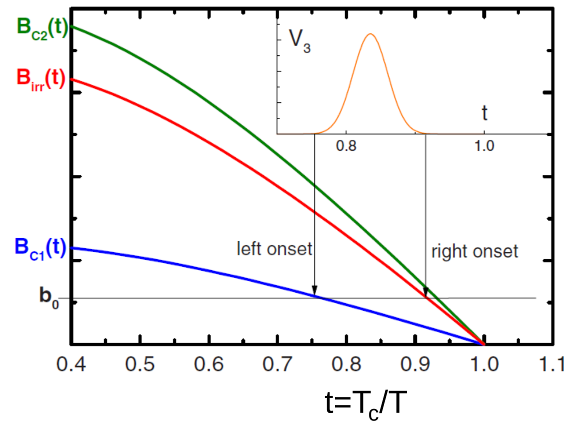

- large sample ensures operation in Bean limit
- use that V3~H* in the Bean limit
- V3 is zero in the Meissner regime and above the irrevsibility line in the flux flow regime

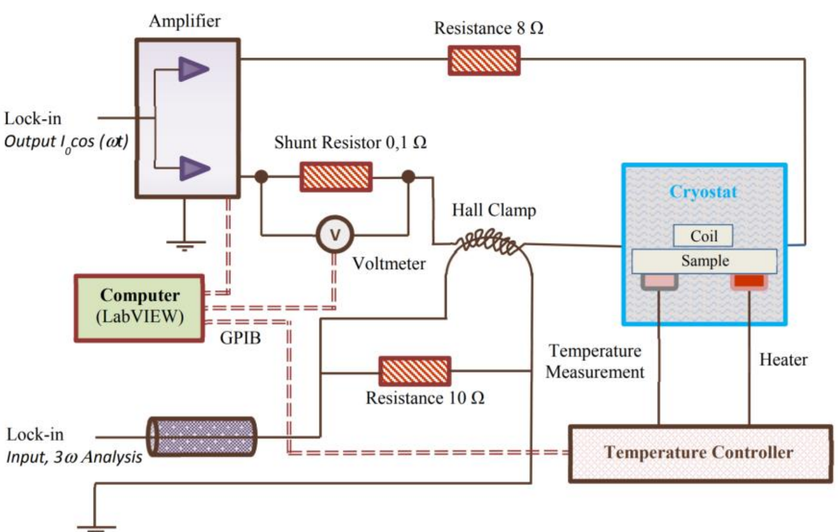

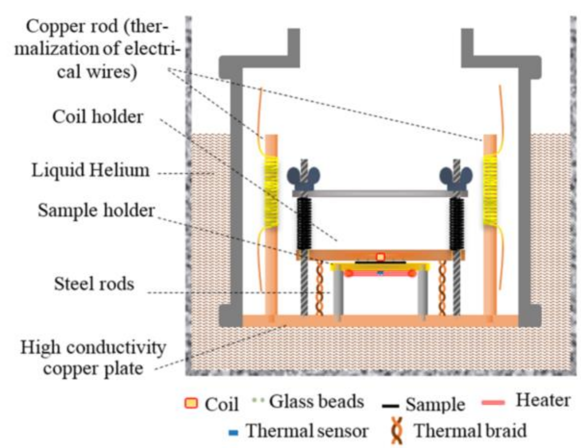

measure third harmonic, V3>0 signifies non-linear response to excitation

Conclusion

- **An overview of a selection of characterisation methods was given**
- **Focus on quadrupole resonator and measurements**
- **Introduction to microwave spectroscopy/microscopy**
- **DC magnetization measurements**